BJ www.biochemj.org

BJ Disease

Biochem. J. (2012) **444**, 515–527 (Printed in Great Britain) doi:10.1042/BJ20112019

online data

Interleukin-6 counteracts therapy-induced cellular oxidative stress in multiple myeloma by up-regulating manganese superoxide dismutase

Charles O. BROWN*[1], Kelley SALEM*[1], Brett A. WAGNER*, Soumen BERA*, Neeraj SINGH*, Ajit TIWARI†, Amit CHOUDHURY†, Garry R. BUETTNER* and Apollina GOEL*[2]

*Free Radical and Radiation Biology Program, Department of Radiation Oncology, University of Iowa, Iowa City, IA 52242, U.S.A., and †Department of Anatomy and Cell Biology, The Holden Comprehensive Cancer Center, University of Iowa, Iowa City, IA 52242, U.S.A.

IL (interleukin)-6, an established growth factor for multiple myeloma cells, induces myeloma therapy resistance, but the resistance mechanisms remain unclear. The present study determines the role of IL-6 in re-establishing intracellular redox homoeostasis in the context of myeloma therapy. IL-6 treatment increased myeloma cell resistance to agents that induce oxidative stress, including IR (ionizing radiation) and Dex (dexamethasone). Relative to IR alone, myeloma cells treated with IL-6 plus IR demonstrated reduced annexin/propidium iodide staining, caspase 3 activation, PARP [poly(ADP-ribose) polymerase] cleavage and mitochondrial membrane depolarization with increased clonogenic survival. IL-6 combined with IR or Dex increased early intracellular pro-oxidant levels that were causally related to activation of NF-κB (nuclear factor κB) as determined by the ability of *N*-acetylcysteine to suppress both pro-oxidant levels and NF-κB activation. In myeloma cells, upon combination with hydrogen peroxide treatment, relative to TNF (tumour necrosis factor)-α, IL-6 induced an early perturbation in reduced glutathione level and increased NF-κB-dependent MnSOD (manganese superoxide dismutase) expression. Furthermore, knockdown of MnSOD suppressed the IL-6-induced myeloma cell resistance to radiation. MitoSOX Red staining showed that IL-6 treatment attenuated late mitochondrial oxidant production in irradiated myeloma cells. The present study provides evidence that increases in MnSOD expression mediate IL-6-induced resistance to Dex and radiation in myeloma cells. The results of the present study indicate that inhibition of antioxidant pathways could enhance myeloma cell responses to radiotherapy and/or chemotherapy.

Key words: dexamethasone, interleukin-6, manganese superoxide dismutase (MnSOD), multiple myeloma, nuclear factor κB (NF-κB), radiation therapy.

INTRODUCTION

MM (multiple myeloma) is a human B-cell neoplasm that invariably shows an aggressive course in the clinic. Of the various secreted cytokines, paracrine and autocrine regulation by IL (interleukin)-6 plays a particularly important role in myeloma cell proliferation and chemoresistance; high expression levels are associated with aggressive disease and poor survival rates [1]. IL-6 has been shown to induce superoxide ($O_2^{\bullet -}$) production in neutrophils, monocytes [2] and neuronal cells [3]. Paradoxically, IL-6 can induce adaptive responses to oxidative stress in normal tissues by protecting pulmonary alveolar cells from hydrogen peroxide (H_2O_2)-induced cell death and preventing reperfusion injury in rats [4]; transgenic mice overexpressing IL-6 in lungs show resistance to hyperoxia [5]. Despite the increasing evidence that IL-6-induced pro-oxidant production could confer an adaptive response in normal tissues, the relationship between IL-6-mediated resistance to oxidative stress and myeloma cell resistance to therapy is unknown.

In comparison with normal tissues, cancer cells thrive in a pro-oxidant environment and are tolerant to oxidative stress [6]. Indeed, MM patients show increased lipid peroxidation and lower levels of antioxidant enzymes in plasma and erythrocytes [7–10]. MnSOD [manganese SOD (superoxide dismutase)] plays a major role in maintaining cellular antioxidant capacity [11,12]. A role for MnSOD in MM progression can be postulated as: (i) mice lacking a copy of the *Sod2* gene show an increased incidence of spontaneous B-cell lymphomas [13]; and (ii) myeloma cells express MnSOD protein at low levels [14,15]. NF-κB (nuclear factor κB), a redox-regulated transcription factor [16], plays a central role in regulating the growth and survival of MM [17]. Cytokines, such as TNF (tumour necrosis factor)-α and IL-1β, have been shown to increase pro-oxidant production, NF-κB-driven induction of *SOD2* mRNA and the enzymatic activity of MnSOD [18,19].

In the present study we show that IL-6 treatment augments radiotherapy- and Dex (dexamethasone)-induced early pro-oxidant levels in myeloma cells. An IL-6-induced resistance to IR (ionizing radiation) and Dex treatment was rendered by NF-κB-driven MnSOD expression. These results support the hypothesis that inhibition of antioxidant pathways could mitigate IL-6-induced adaptive responses to radiotherapy and/or chemotherapy in myeloma cells.

Abbreviations used: BM, bone marrow; CF, cleaved fragment; Dex, dexamethasone; DHE, dihydroethidium; E^+, ethidium cation; GPx, glutathione peroxidase; H_2DCF-DA, 2′,7′-dichlorodihydrofluorescein diacetate; ICCM, irradiated cell conditioned medium; IκB, inhibitor of NF-κB; IL, interleukin; IR, ionizing radiation; JC-1, 5,5′,6,6′-tetrachloro-1,1′,3,3′-tetraethylbenzimidazolylcarbocyanine iodide; KD, knockdown; MFI, mean fluorescence intensity; MM, multiple myeloma; MOI, multiplicity of infection; MnSOD, manganese superoxide dismutase; MTT, 3-(4,5-dimethylthiazol-2-yl)-2,5-diphenyl-2*H*-tetrazolium bromide; NAC, *N*-acetylcysteine; NBD, NEMO (NF-κB essential modulator)-binding domain; NF-κB, nuclear factor-κB; NSF, normalized survival fraction; 2-OH-E^+, 2-hydroxyethidium; PARP, poly(ADP-ribose) polymerase; PEG–SOD, poly(ethylene glycol)-conjugated superoxide dismutase; PI, propidium iodide; qPCR, quantitative PCR; RLU, relative luciferase units; ROS, reactive oxygen species; shRNA, small hairpin RNA; SOD, superoxide dismutase; TNF, tumour necrosis factor; Z-LEHD-FMK, benzyloxycarbonyl-Leu-Glu-His-DL-Asp-fluoromethylketone; Z-VAD-FMK, benzyloxycarbonyl-Val-Ala-DL-Asp-fluoromethylketone.

[1] These authors contributed equally to this study.

[2] To whom correspondence should be addressed (email apollina-goel@uiowa.edu).

EXPERIMENTAL

Cell culture

The human BM (bone marrow) stromal cell line HS-5 (CRL-11882) and myeloma cell line RPMI-8226 (8226, CCL-155) were obtained from A.T.C.C. The MM.1S myeloma cell line was from Dr Steve Rosen (Feinberg School of Medicine, Northwestern University, Chicago, IL, U.S.A.) and HBME-1, a human BM endothelial cell line, was from Dr Kenneth Pienta (Department of Internal Medicine, University of Michigan, Ann Arbor, MI, U.S.A.). All cell lines were grown in RPMI complete medium as described previously [20]. For most experiments, cells were pre-treated for 6 h with IL-6 (50 ng/ml, R&D Systems), prior to exposure to IR (6 Gy, delivered using a Cs-137 source at a dose rate of 0.83 Gy/min), and post-cultured for different times without or with IL-6.

Clonogenic survival assay

Cells were seeded overnight in complete medium in 24-well plates (1×10^5 cells/well), and then treated with IL-6 and/or IR. For adherent cells (HS-5 and HBME-1), 100 cells/well were seeded in six-well plates (in triplicate) and cultured for 7 days. Colonies were fixed with 75 % methanol/25 % acetic acid, stained with 0.2 % Coomassie Blue solution and the number of clonogenic cells was assessed [21]. Clonogenicity of myeloma cells was determined using the limiting dilution method [22]. Plating efficiency and survival fractions were calculated as described previously [20]. For each cell population, the NSF (normalized survival fraction), relative to the number of untreated control cells, was calculated.

Measurement of apoptosis

Viability and induction of cell death (early and late apoptosis/necrosis) were examined by annexin-V–FITC/PI (propidium iodide) dual staining of cells (Cayman Chemical) followed by flow cytometric analysis according to previously published methods [23].

Apoptosis was also measured by a caspase 3 fluorescence assay (Cayman Chemical) as described previously [20]. Caspase 3 activity is expressed as units/mg of total protein.

Measurement of mitochondrial membrane potential was performed using the JC-1 (5,5′,6,6′-tetrachloro-1,1′,3,3′-tetraethylbenzimidazolylcarbocyanine iodide) dye (Molecular Probes, Invitrogen) as described previously [20]. The cationic dye JC-1 accumulates and aggregates in intact mitochondria, emitting a bright red fluorescence, whereas, upon disruption of the mitochondrial membrane potential, the monomeric dye emits green fluorescence in the cytoplasm. Briefly, cells were pre-treated with conditioned medium from irradiated HS-5 cells [ICCM (irradiated cell conditioned medium), 6 Gy collected 24 h post-IR] or IL-6 (1, 2.5, 10 or 50 ng/ml) for 6 h followed by irradiation. At 24 h post-treatment, cells were incubated with JC-1 dye (200 nM for 30 min) at 37 °C in the dark and read using a fluorescent plate reader (Tecan) with excitation and emission wavelengths set at 485 and 595 nm respectively for red fluorescence, and 485 and 535 nm respectively for green fluorescence. For each condition, triplicate samples were run, fluorescent readings were corrected for background, and the ratio of red signal to green signal was calculated.

Immunoblotting

Protein immunoblotting was performed according to standard protocols as described previously [20,23,24]. Cells were seeded in complete medium in six-well culture plates (1×10^6 cells/well) followed by IL-6 treatment and/or irradiation. Alternatively, cells were treated for 2 h with 50 μM Z-LEHD-FMK (benzyloxycarbonyl-Leu-Glu-His-DL-Asp-fluoromethylketone; Sigma), ICCM, or anti-IL-6Rα antibody (0.2 μg/ml, R&D Systems, 2 h pre-treatment of cells before addition of ICCM). Total cell lysate was prepared 24 h post-irradiation. For this, cells were lysed using 1 % Nonidet P40 buffer (50 mM Tris/HCl, pH 7.4, 250 mM NaCl, 5 mM EDTA, 50 mM NaF, 1 mM Na_3VO_4 and 0.02 % NaN_3, 30 min on ice), centrifuged at 14 000 ***g*** for 10 min, and supernatants were collected. Protein concentrations were determined using the Bio-Rad dye reagent (Bio-Rad Laboratories), and 20–50 μg of protein per lane was separated by SDS/PAGE (12.5% gels) and transferred to PVDF membranes. Non-specific binding was blocked with 5 % (w/v) non-fat dried skimmed milk powder in TBST buffer (4 mM Tris base, 100 mM NaCl, pH 7.5, and 0.1 % Tween 20) and incubated overnight at 4 °C, with primary antibodies against MnSOD, PARP [poly(ADP-ribose) polymerase]-CF (cleaved fragment), IκBα (inhibitor of NF-κB α), tubulin (all from Cell Signaling Technology) or GAPDH (glyceraldehyde-3-phosphate denydrogenase, Imgenex), and then incubated with secondary antibody for 1 h at room temperature (25°C). Blots were developed by enhanced chemiluminescence assay (Thermo Scientific). Bands were visualized by autoradiography and then analysed using Image J 1.38x software (http://rsbweb.nih.gov/ij/index.html). For illustrations, Adobe Photoshop CS4 was used where Figures were converted into greyscale, cropped, and then contrast-corrected using Photoshop's 'Auto Contrast' tool.

Detection of intracellular ROS (reactive oxygen species)

Intracellular oxidants, such as ROS, were detected using the oxidation-sensitive fluorescent probe dye carboxy-H_2DCF-DA (carboxy-2′,7′-dichlorodihydrofluorescein diacetate, Invitrogen) [20]. Cells were seeded overnight in 96-well plates and treated for 2 h with IL-6 (1, 2.5, 10 or 50 ng/ml), IL-6 (50 ng/ml) plus irradiation, TNF-α (2.5 ng/ml), IL-1β (1 ng/ml), Dex (1 μM) or Dex plus irradiation. Specific wells were pre-treated with NAC (*N*-acetylcysteine) before treatments. Samples were incubated with H_2DCF-DA (10 μg/ml, 30 min) and fluorescence was measured (Tecan; $\lambda_{ex} = 495$ nm, $\lambda_{em} = 530$ nm).

DHE (dihydroethidium) was used to measure IL-6, IR and/or Dex-induced formation of intracellular oxidants. Specifically, myeloma cells were incubated with DHE (10 μM, Invitrogen) at 37 °C for 30 min (Phenol-Red-free RPMI 1640 medium containing 5 mM pyruvate) followed by treatment with IL-6 or IR (0.5, 1 or 2 h), IL-6 plus IR (2 h) or Dex (2 h). Formation of 2-OH-E^+ (2-hydroxyethidium) was preferentially detected using flow cytometry with $\lambda_{ex} = 405$ nm and $\lambda_{em} = 585$ nm [25]. For each sample, the MFI (mean fluorescence intensity) of 10 000 live cells was analysed and corrected for autofluorescence against the control untreated cells.

Changes in the mitochondrial oxidant production were measured using MitoSOX Red staining (5 mM for 15 min at 37 °C, Invitrogen) followed by flow cytometry ($\lambda_{ex} = 488$ nm and $\lambda_{em} = 585$ and 542 nm) [26]. The specificity of DHE and MitoSOX staining was confirmed using PEG–SOD [poly (ethylene glycol)-conjugated SOD; 100 units/ml, 2 h before treatments] or antimycin A treatment (100 μM for 2 h). Alternatively, myeloma cells were treated without or with Z-VAD-FMK (benzyloxycarbonyl-Val-Ala-DL-Asp-fluoromethylketone; Sigma, 100 μM for 2 h [23]) followed by IL-6 and/or IR treatments and cultured for 36 h in 96-well plates. Cells were washed with PBS (137 mM NaCl, 10 mM phosphate and 2.7 mM

KCl, pH 7.4) and incubated with MitoSOX Red (5 μM, final concentration) at 37 °C for 10 min. Fluorescence intensity was measured at 510/580 nm using a plate reader (Tecan). The experiment was repeated twice, and run in triplicate for each treatment condition. The mean intensity of MitoSOX fluorescence was normalized with that in control untreated cells, and the fold change in intensity in the context of treatments was calculated. The presence of intracellular 2-OH-E^+ was also verified using HPLC following the method of Zielonka et al. [25] and is described in the Supplementary Experimental section (at http://www.BiochemJ.org/bj/444/bj4440515add.htm).

For confocal microscopy, at 36 h post-treatment, cells were suspended in PBS containing MitoSOX Red (5 μM) and MitoTracker Green (50 nM, Invitrogen), and incubated at 37 °C for 30 min. Cells were gently washed with warm PBS and live imaging was performed using a Leica spinning-disk confocal microscope equipped with a Hamamatsu EM-CCD (charged-coupled-device) digital camera (Hamamatsu Photonics) and the 'Metamorph' image acquisition and processing software (Molecular Devices). All images were acquired using a 63× 1.3 NA (numerical aperture) objective. In these experiments, all photomicrographs were exposed and processed identically for a given fluorophore. Images were corrected for background fluorescence using unlabelled specimens. For double-labelling experiments, control samples were labelled identically with the individual fluorophores, and exposed identically with the dual-labelled samples at each wavelength, to verify that there was no signal crossover from different emission channels at the exposure settings used.

GSH assay

Cells were seeded into six-well plates (1×10^5/ml) in complete medium for 12 h, and were either left untreated or were treated with IL-6 (2.5 or 50 ng/ml) or TNF-α (2.5 or 10 ng/ml), for 4, 10 or 24 h. At completion of the treatment time, cells were pelleted (800 ***g*** for 5 min at 4 °C), rinsed once with PBS and resuspended in metaphosphoric acid (5 min at room temperature, 100 mg/ml; Sigma). The supernatant was collected by centrifugation (18 000 ***g*** for 3 min), neutralized with 4 M triethanolamine (Sigma) and used to estimate total GSH (Cayman Chemical). Each sample (20 μl) was diluted in 2× Mes buffer (0.4 M Mes, 0.1 M phosphate and 2 mM EDTA, pH 6.0) and absorbance was measured at 5 min intervals for 30 min (Tecan, 405–414 nM). The GSH assay kit uses an enzymatic recycling method, measuring the TNB (5-thio-2-nitrobenzoic acid) generated in the presence of GSH reductase to estimate total GSH in the sample. The protein pellet was dissolved in 1 M NaOH and used for protein estimation. All assessments of glutathione levels were normalized to the protein content and are expressed as nmoles of total GSH/mg of protein.

Adenoviral transduction

Cells (3×10^5 cells/well) were seeded overnight in 24-well plates in complete medium. Recombinant adenovirus was added in serum-free medium, centrifuged for 30 min at 25 °C, and then incubated for 2 h at 37 °C. Cells were allowed to recover for 48 h in complete medium. For all cell lines, the adenovirus transduction efficiency was >80 %, as assessed by measurement of Ad-CMV-GFP reporter gene expression (results not shown). Adenoviruses expressing human MnSOD cDNA (Ad-MnSOD), control (Ad-CMV), Ad-IκBα(S32A/S36A) (also referred to as Ad-IκBα-DN), and NF-κB-driven luciferase reporter (Ad-NF-κB Luc) were obtained from the Gene Transfer Vector Core at the University of Iowa. For all recombinant adenoviral constructs, a MOI (multiplicity of infection) of 100 was used, except for Ad-IκBα-DN, where a MOI of 10 was used.

Reporter gene assay

Cells were transduced with Ad-NF-κB Luc for 48 h and then treated with IL-6 (50 ng/ml), TNF-α (2.5 ng/ml), H_2O_2 (100 μM) and/or IR. At 4 h post-irradiation, the cells were lysed in 1 % Triton X-100 buffer (50 mM Tris, 150 mM NaCl, 1 % Triton X-100 and 10 mM EDTA, pH 7.2), and luciferase was measured using the Luc assay (Promega). To assess whether IR- and/or IL-6-induced redox changes up-regulate Ad-NF-κB Luc activity, MM.1S cells were pre-treated with or without NAC (10 mM for 1 h) and stimulated with IL-6 and/or IR for 4 h followed by the Luc assay. The level of reporter gene expression was presented as RLU (relative luciferase units)/mg of total protein.

Generation of stable *SOD2* KD (knockdown) myeloma cells

An shRNA (small hairpin RNA) subcloned into the pLKO.1 lentivirus (Open Biosystems, RHS4533) was used to generate myeloma cells in which the *SOD*2 gene was stably knocked down. Virus particles were generated by co-transfecting the *SOD*2 shRNA-expressing plasmid, envelope plasmid (pMD2.G), and packaging plasmid (pCMV-dR8.91) into HEK (human embryonic kidney)-293T cells using Lipofectamine™ 2000 (Invitrogen). Virus-containing supernatants were collected at 48 h, filtered through a 0.45 μM filter, and used to transduce MM.1S or 8226 cells in the presence of polybrene (8 μg/ml, Sigma). At 24 h, the medium was replaced and the stable cell population was enriched with puromycin (2 μg/ml) for 2 weeks. The new cell lines were expanded, and MnSOD KD was confirmed by immunoblotting and activity assays.

MnSOD activity assay

MnSOD activity in whole-cell lysates was measured after treatment with IL-6 and/or IR, in the absence or presence of NBD [NEMO (NF-κB essential modulator)-binding domain; 50 μM for 2 h; Imgenex) peptide or Ad-IκBα(S32A/S36A), using a kit (Cayman Chemical). This assay is based on tetrazolium salt-based detection of $O_2^{\bullet-}$ generated by xanthine oxidase and hypoxanthine. One unit of MnSOD is defined as the amount of protein needed to achieve 50 % inhibition of $O_2^{\bullet-}$-mediated reduction of the tetrazolium salt in the presence of potassium cyanide (2.5 mM for 30 min pre-incubation prior to running the assay). The absorbance was read at 450 nm and enzyme activities were expressed as specific activity (units of activity/mg of total protein).

qPCR (quantitative PCR)

Cells were incubated with IL-6 (50 ng/ml), TNF-α (2.5 ng/ml) or IL-1β (1 ng/ml), and cultured for 10 h. Alternatively, cells were pre-treated with IL-6, irradiated and then further cultured for 10 h. Total RNA was isolated using a Qiagen RNeasy kit (Qiagen) and quantified. cDNA was synthesized from 800 ng of total RNA, using the iScript cDNA synthesis kit (Bio-Rad Laboratories). Thermocycler conditions included a 5 min incubation at 25 °C, a 30 min incubation at 42 °C, and a 5 min incubation at 85 °C. The cDNAs were subjected to qPCR analysis with the following 5′→3′ primers (sense and antisense respectively): SOD2, GCCTGCACTGAAGTTCAATGG and GCTTCCAGCAACTCCCCTTT, amplicon length 105 bp; catalase, TTCGGTTCTCCACTGTTGCTG and AATTTCACTGCAAACCCACGA, amplicon length 76 bp; GPx (glutathione peroxidase)-1, AACGATGTTGCCTGGAACTTTG and GAAGCGGCGGCTGTACCT,

amplicon length 79 bp; and human 18S, CCTTGGATGTGGTAGCCGTTT and AACTTTCGATGGTAGTCGCCG, amplicon length 105 bp. Primers were designed using the Primer Express software (Applied Biosystems). The assay was performed in a 96-well optical plate, with a final reaction volume of 20 μl, including synthesized cDNA (20 ng), oligonucleotide primers (100 μM each), and 2× SYBR Green/ROX PCR master mix (Bio-Rad Laboratories). Samples were run on an ABI PRISM Sequence Detection System (model 7000, Applied Biosystems). PCR conditions were 50 °C for 2 min, 95 °C for 2 min and 30 s, 95 °C for 15 s, and 60 °C for 1 min for 40 cycles. Results were analysed using the ABI PRISM 7000 SDS software. The denaturation and annealing steps were carried out for 40 cycles to determine the threshold cycle (C_T) values for all of the genes analysed. Samples were checked for non-specific products or primer/dimer amplification by melting curve analysis. The C_T values for the target genes in all of the samples (analysed in triplicate) were normalized on the basis of the abundance of the 18S transcript, and the fold difference (relative abundance) was calculated using the formula $2^{-\Delta\Delta}C_T$ and was plotted as the mean ($n = 3$).

Statistical analysis

Results in histograms represent means ± S.D. Statistical analysis using Student's *t* test or one-way ANOVA followed by Student-Newman Keuls *t* test were performed. $P < 0.05$ was considered to be statistically significant.

RESULTS

IL-6 confers radioresistance in myeloma cells

In our previous study, using myeloma–BM stromal cell co-culture, we showed that paracrine IL-6 inhibits irradiation-mediated killing of myeloma cells [20]. To determine whether addition of exogenous IL-6 inhibits myeloma cell killing by irradiation, clonogenic cell survival assays were performed. Irradiation alone reduced the clonogenic survival of myeloma cells and BM accessory cells by 40–50 % (Figure 1A). Notably, IL-6 plus IR increased clonogenicity of myeloma cells but did not affect the radiosensitivity of HS-5 or HBME-1 cells (Figure 1A), suggesting that IL-6 induces radioresistance in myeloma cells. Next, various parameters indicative of apoptosis were evaluated at 24 h post-IR without or with treatment with IL-6. In annexin V/PI staining, IL-6 reduced IR-induced apoptosis from 43 % to 17 % and 22 % to 8 % in MM.1S and 8226 cells respectively (Figure 1B). The pan-caspase inhibitor Z-VAD-FMK significantly interfered with IR- or IL-6 plus IR-induced apoptosis (results not shown). IR led to 2.4-fold and 1.3-fold increases in the activation of caspase 3 in the MM.1S and 8226 cells respectively, which was inhibited by IL-6 (Figure 1C). Also, IL-6 inhibited the p85 PARP cleavage induced by IR (Figure 1D, panel i). Since the HS-5 cell line has been shown to secrete IL-6 [27], we next determined whether the conditioned medium from irradiated HS-5 cells (ICCM) similarly protects myeloma cells from IR-induced apoptosis, as seen with the addition of exogenous IL-6. Using an ELISA assay, the IL-6 concentration in the HS-5 culture supernatant with 6 Gy of radiation treatment at 24 h was detected as 3.5 ± 0.2 ng/ml relative to 1.9 ± 0.1 ng/ml for untreated cells. For MM.1S and 8226 cells, irradiation resulted in PARP cleavage at 24 h, which was blocked by pre-treatment with a caspase 9 inhibitor (Figure 1D, panel ii). Notably, in both MM.1S and 8226 cells, radiation-induced PARP cleavage at 24 h was partially blocked by 6 h of pre-incubation with ICCM and blocking of the ligand-binding IL-6 receptor α-chain abrogated the radioprotective effect of ICCM on myeloma cells (Figure 1D, panel ii). To further confirm that radiation-induced apoptosis is prevented by ICCM or exogenous IL-6, the relative changes in mitochondrial membrane potential were measured using JC-1 dye. At 24 h post-treatment, both MM.1S and 8226 cell lines showed a drop in mitochondrial membrane potential (indicated by a decrease in the ratio of red signal to the green signal) with irradiation, which was significantly inhibited by pre-treatment with ICCM or IL-6 (Figure 1E). To determine whether exogenous IL-6 protects IR-induced myeloma cell apoptosis in a dose-dependent fashion, cells were treated with IL-6 (1, 2.5, 10 or 50 ng/ml for 2 h) followed by irradiation, and JC-1 staining was performed at 24 h. For both MM.1S and 8226 cells, all IL-6 concentrations, except 1 ng/ml, inhibited IR-induced mitochondrial depolarization (Figure 1F). Cumulatively, Figure 1 shows that exogenous IL-6 at concentrations of 2.5, 10 or 50 ng/ml protects myeloma cells from irradiation-induced apoptosis.

IL-6 stimulates ROS generation by IR and Dex in myeloma cells

We have previously shown that irradiation induces ROS production in myeloma cells [20]. Given that IL-6 can also increase intracellular $O_2^{\bullet -}$ levels [2,3], we next determined whether IL-6 treatment alters irradiation-mediated perturbations in pro-oxidant levels in myeloma cells. Treatment with IL-6 or IR for 2 h increased H_2DCF-DA oxidation, and IL-6 plus IR enhanced this response (Figure 2A). The effects of IL-6 and/or IR on H_2DCF-DA oxidation were abrogated with treatment with the thiol antioxidant NAC (Figure 2A). To assess whether combined treatment with IL-6 plus IR results in an increased steady-state level of intracellular pro-oxidants (presumably $O_2^{\bullet -}$) at 2 h, the oxidation-sensitive DHE probe was used and flow cytometry was performed as described by Robinson et al. [28]. In MM.1S cells, IL-6 and IR treatment resulted in a 2.2 ± 0.4- and 1.7 ± 0.2-fold increase in DHE oxidation relative to the control, which was set to 1 (Figure 2B). Notably, combined treatment of IL-6 plus IR resulted in a 2.4 ± 0.2-fold increase in DHE oxidation, which was higher compared with treatment with IL-6 or IR (Figure 2B). A time kinetic study of DHE oxidation in MM.1S cells by IL-6 or IR treatment showed that IL-6 steadily increased DHE oxidation for 2 h and IR induced DHE oxidation for 2 h, yet a maximum DHE oxidation was noted at 1 h post-irradiation (Supplementary Figures S1A and S1B respectively at http://www.BiochemJ.org/bj/444/bj4440515add.htm). Since a lower concentration of IL-6 was detected in the supernatant of irradiated HS-5 cells, a dose-dependent production of pro-oxidants with the addition of exogenous IL-6 was investigated. For MM.1S and 8226 cells, IL-6 treatment (2.5, 10 or 50 ng/ml for 2 h) resulted in an increased H_2DCF-DA oxidation (Supplementary Figure S1C), demonstrating that both physiological and high levels of IL-6 treatments increase the steady-state levels of intracellular pro-oxidants in myeloma cells.

Previous reports have shown a limited specificity of hydroethidine-based fluorigenic probes for detecting intracellular $O_2^{\bullet -}$ [25,26,29]. To corroborate DHE oxidation results, HPLC analysis of $O_2^{\bullet -}$-specific DHE oxidation was performed. IL-6 treatment did not result in increased oxidation of DHE to 2-OH-E^+ when compared with untreated controls (results not shown). When 8226 cells were treated with antimycin A, which inhibits complex III of the mitochondrial electron transport chain thereby generating $O_2^{\bullet -}$, HPLC analysis predominantly showed the production of E^+ (ethidium cation) (Supplementary Figure S2 at http://www.BiochemJ.org/bj/444/bj4440515add.htm). Quantitative analysis of the one- and two-electron oxidation products of DHE with antimycin A treatment indicate that DHE oxidation

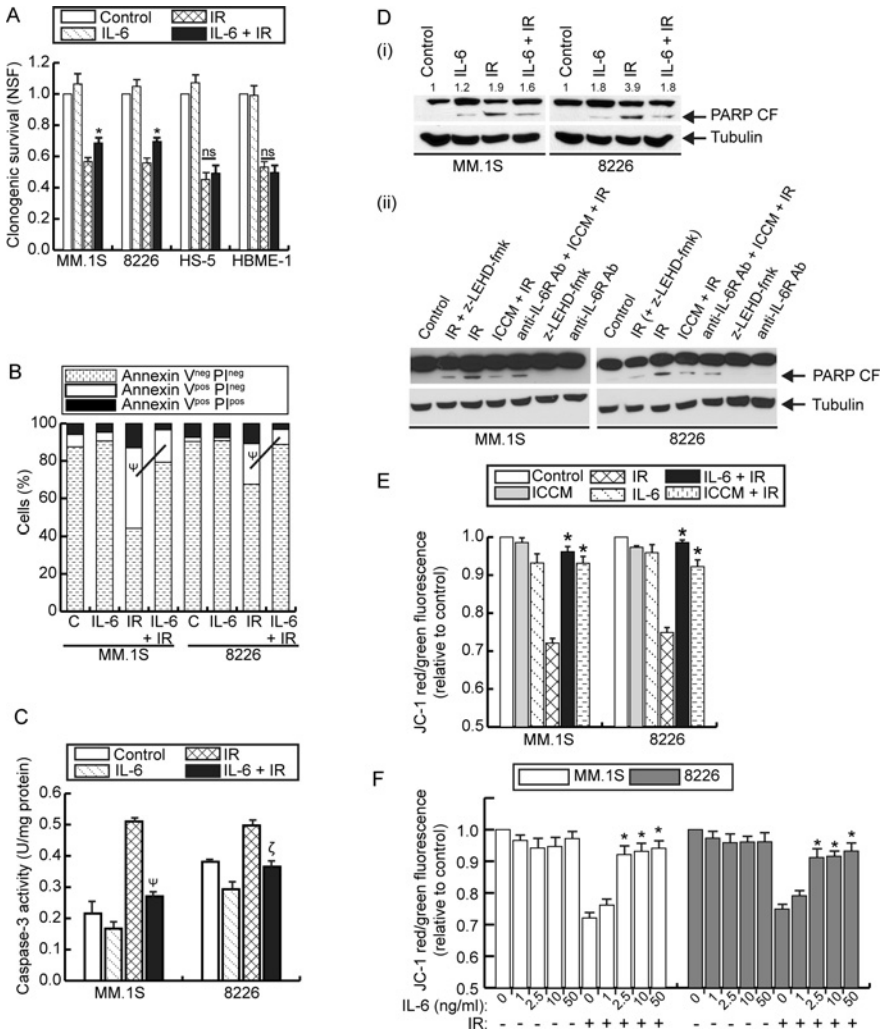

Figure 1 IL-6 protects myeloma cells from irradiation-induced apoptotic cell death

(**A**) Clonogenic survival of myeloma (MM.1S, 8226) or BM accessory cells (HS-5, HBME-1) cells treated with IL-6 (50 ng/ml) and/or IR (6 Gy) and normalized to untreated control cells. Values represent the mean of three replicates ± S.D. $^*P < 0.05$ compared with IR; ns, not significant. (**B**) Percentage of viable, apoptotic and necrotic/late apoptotic cell populations in myeloma cells treated with IL-6 (50 ng/ml) and/or IR and assessed by flow cytometry at 24 h. Results shown are from one experiment, and representative of three independent experiments. $^\Psi P < 0.001$. neg, negative; pos, positive. (**C**) Caspase 3 activity in myeloma cells treated with IL-6 (50 ng/ml) and/or IR at 24 h. Values represent the mean of three replicates ± S.D. $^\Psi P < 0.001$ and $^\zeta P < 0.01$ compared with IR. (**D**) Representative levels of PARP-CF and loading control (tubulin) in whole-cell lysates of myeloma cells at 24 h (i) treated with IL-6 (50 ng/ml) and/or IR or (ii) in control or irradiated myeloma cells treated with the caspase 9 inhibitor (Z-LEHD-FMK), ICCM and/or IL-6Rα-blocking antibodies. Band intensities relative to respective tubulin controls are shown above each blot. Immunoblotting results are from one experiment, and representative of two independent experiments. JC-1 fluorescence at 24 h in myeloma cells pre-treated with (**E**) ICCM or IL-6 (50 ng/ml) followed by irradiation, or (**F**) IL-6 (0, 1, 2.5, 10 or 50 ng/ml) followed by irradiation. The average JC-1 red/green fluorescent ratio relative to the control (non-irradiated with medium alone) is shown. $^*P < 0.01$ compared with IR. Two experiments were conducted and results from one experiment are shown.

in myeloma cells leads to approximately 100-fold more E^+ than 2-OH-E^+. At this stage, it remains speculative whether the chemistry of DHE and 2-OH-E^+ and the formation of other oxidation products, e.g. dimers of E^+ or 2-OH-E^+, or even mixed dimers of E^+ and 2-OH-E^+, results in an 'under-reporting' of formation of 2-OH-E^+. Nevertheless, the results using oxidation-sensitive fluorescent probes (H_2DCF-DA and DHE) suggest that IL-6 treatment results in increased intracellular levels of early pro-oxidant production in myeloma cells that is further augmented with irradiation.

We have previously reported that Dex treatment exerts an anti-myeloma effect by promoting the production of $O_2^{\bullet -}$ and H_2O_2 [20]. We next determined whether the protective role of IL-6 on IR-mediated myeloma cell killing could be extended to Dex-induced therapy resistance in MM. Treatment with Dex increased H_2DCF-DA oxidation, and this effect was enhanced by the combination of IL-6 and Dex (Figure 2C). A kinetic study over time showed a steady increase in DHE oxidation with Dex treatment with approximately a 2-fold increase in DHE oxidation at 2 h (Supplementary Figure S3A at http://www.BiochemJ.org/bj/444/bj4440515add.htm). In the MTT [3-(4,5-dimethylthiazol-2-yl)-2,5-diphenyl-2*H*-tetrazolium bromide] assay, IL-6 significantly inhibited Dex-mediated myeloma cell killing (Supplementary Figure S3B). This is consistent with IL-6 as an established inhibitor of anti-myeloma activity of glucocorticoids, including Dex [1], and agrees with the observed IL-6-induced radioresistance in myeloma cells (Figure 1).

Besides IL-6, TNF-α and IL-1β promote the survival and proliferation of myeloma cells, and also trigger pro-oxidant production [30,31]. We therefore measured the levels of pro-oxidant generated in response to TNF-α and IL-1β treatments and compared this with IL-6 exposure. In myeloma cells, TNF-α

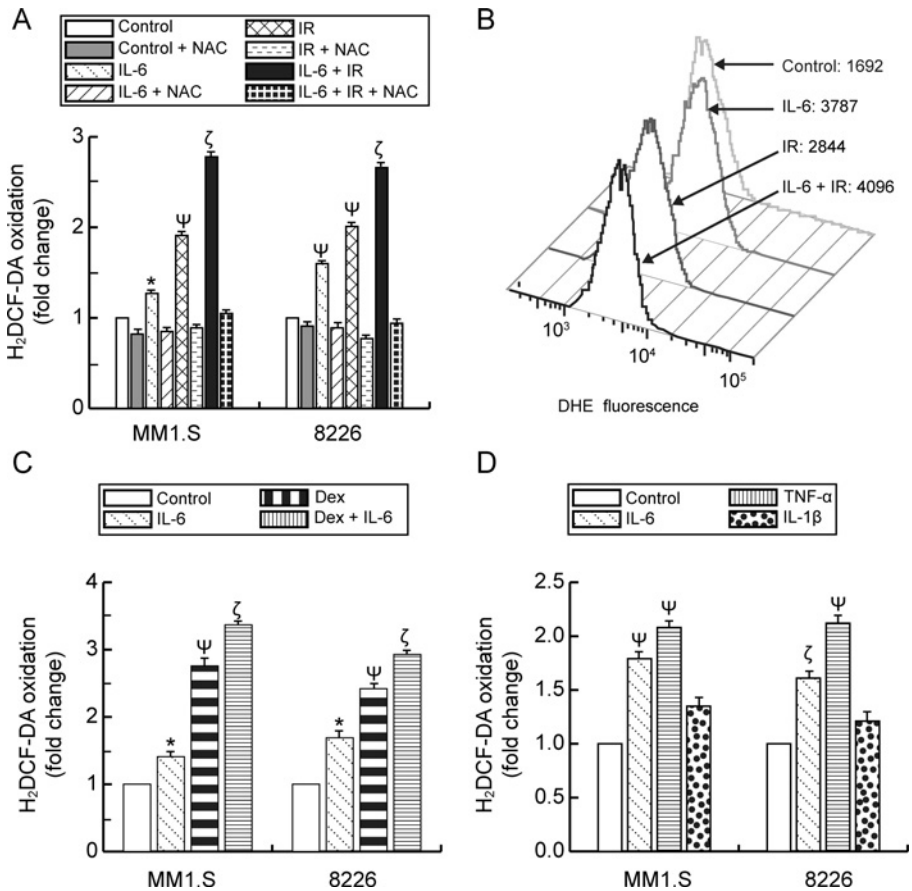

Figure 2 IL-6 increases early steady-state levels of intracellular pro-oxidants generated by radiation or Dex treatment and H_2DCF-DA oxidation by IL-6, TNF-α or IL-1β

(**A**) Myeloma cells were treated with IL-6 (50 ng/ml) and/or IR (without or with NAC) and H_2DCF-DA oxidation was measured at 2 h. $^*P < 0.05$ or $^{\Psi}P < 0.001$ compared with control, $^{\zeta}P < 0.005$ compared with IR treatment alone. (**B**) MM.1S cells were treated with IL-6 (50 ng/ml) and/or IR and DHE oxidation was measured after 2 h by flow cytometry. Histograms with MFI values are shown from one experiment, and are representative of two independent experiments. For each histogram, the *x* axis and *y* axis show the percentage of cells and DHE oxidation respectively. (**C**) Myeloma cells were treated with IL-6 (50 ng/ml) and/or Dex, and H_2DCF-DA was measured at 2 h. The values represent the means $\pm$ S.D. from three replicates and are normalized to the untreated control. $^*P < 0.05$ or $^{\Psi}P < 0.001$ compared with the control, $^{\zeta}P < 0.05$ compared with Dex treatment alone. (**D**) H_2DCF-DA oxidation after 2 h in myeloma cells treated with IL-6 (50 ng/ml), TNF-α (2.5 ng/ml) or IL-1β (1 ng/ml). Means $\pm$ S.D. from three replicates is shown. $^{\Psi}P < 0.005$ or $^{\zeta}P < 0.001$ compared with the control.

induced a more robust ROS production than IL-6, whereas IL-1β only marginally increased the H_2DCF-DA oxidation (Figure 2D). The selected concentrations of IL-6 (50 ng/ml), TNFα (2.5 ng/ml) or IL-1β (1 ng/ml) supported myeloma cell proliferation, as confirmed by the MTT assay (results not shown).

Overall, in myeloma cells, IL-6 treatment was found to increase early pro-oxidant levels and potentiate overall ROS production induced by irradiation or Dex treatments. Strikingly, as seen in Figure 1, IL-6 treatment increased clonogenic survival of myeloma cells and also decreased the cytotoxicity of IR and Dex. Taken together, the results of Figures 1 and 2 show that the elevated early ROS production by combination therapy is not cytotoxic to myeloma cells, and that IL-6 treatment may somehow prime myeloma cells to resist the oxidative stress-induced cell killing.

IL-6 and TNF-α differentially regulate H_2O_2-mediated NF-κB activation, apoptotic cell death and steady-state levels of GSH in myeloma cells

NF-κB is a redox-regulated transcription factor where diverse stimuli that appear to utilize ROS can act as common effectors for activating NF-κB [16]. Since treatment with pro-inflammatory cytokines (TNF-α and IL-6) and anti-myeloma therapeutic agents (IR and Dex) induced early ROS production in myeloma cells, we assessed whether increased pro-oxidant production by these agents was associated with NF-κB activation. Studies were conducted where oxidative stress was produced by H_2O_2 treatment. Similar to IR, H_2O_2 treatment produces different types of ROS, i.e. $O_2^{\bullet -}$, H_2O_2 and hydroxyl radicals, which are capable of damaging DNA, protein and lipid membranes in cells [32]. Myeloma cells were treated with IL-6, TNF-α and/or H_2O_2, and NF-κB activity was measured at 4 h using an adenoviral-delivered NF-κB reporter assay. Relative to IL-6, TNF-α treatment resulted in a more pronounced increase in NF-κB activation (Figure 3A). When cytokine treatment was combined with H_2O_2, an increase in NF-κB activation was noted for IL-6, whereas combination of TNF-α with H_2O_2 resulted in an attenuation of NF-κB activity (Figure 3A).

We next assessed whether TNF-α treatment inhibits myeloma cell death induced by oxidative stressors, as seen for IL-6 when combined with IR or Dex treatments. For this, activated caspase 3, as a biochemical marker of apoptosis, was measured at 24 h in myeloma cells treated with TNF-α or IL-6 in the presence or absence of H_2O_2. In myeloma cells, treatment with H_2O_2 resulted in activation of caspase 3; this was significantly

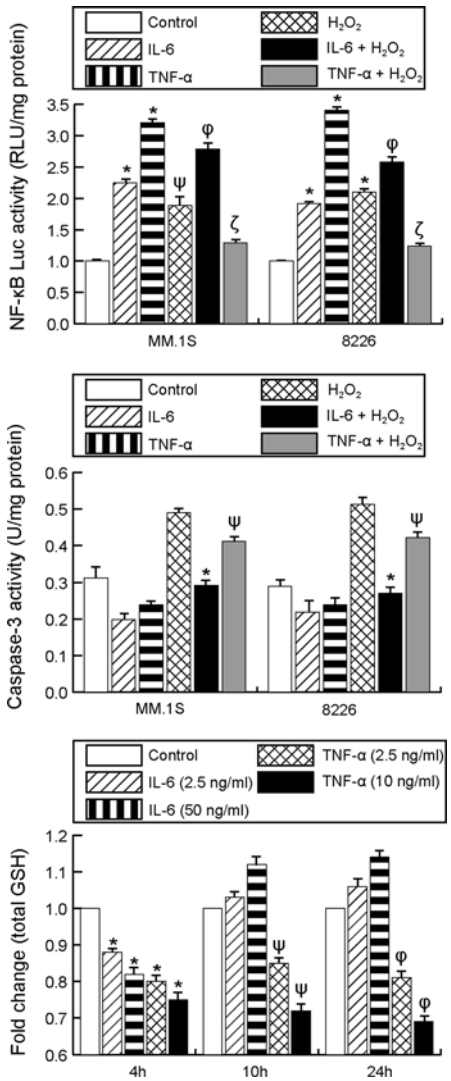

Figure 3 IL-6 and TNF-α differentially regulate H_2O_2-induced-oxidative-stress-mediated NF-κB activation, apoptotic cell death and steady-state levels of GSH in myeloma cells

Myeloma cells were treated with IL-6 (50 ng/ml) or TNF-α (2.5 ng/ml) alone or in combination with H_2O_2 (100 μM) and (top panel) NF-κB-driven luciferase activity was measured at 4 h. Values are depicted as the fold change in mean RLU ± S.D., $n = 3$, normalized to protein concentration. $^{*}P < 0.001$ or $^{\Psi}P < 0.005$ compared with control, $^{\varphi}P < 0.01$ compared with IL-6 or $^{\zeta}P < 0.001$ compared with TNF-α. Middle panel, myeloma cells were treated as in the top panel and caspase 3 activity was measured at 24 h. Values represent averages of three replicates ± S.D. $^{*}P < 0.001$ compared with H_2O_2, $^{\Psi}P < 0.05$ compared with H_2O_2. Bottom panel, intracellular GSH levels in 8226 cells, measured at 4, 10 or 24 h following treatment with IL-6 (2.5 or 50 ng/ml) or TNF-α (2.5 or 10 ng/ml). Total GSH was measured using the spectrophotometric recycling assay and fold change relative to each time point was calculated. Values represent the mean of three runs ± S.D. $^{*}P < 0.001$ compared with the 4 h control, $^{\Psi}P < 0.001$ compared with the 10 h control and $^{\varphi}P < 0.001$ compared with the 24 h control.

blocked by IL-6 treatment, whereas only a slight rescue in H_2O_2-mediated activation of caspase 3 was noted with TNF-α treatment (Figure 3B). Thus TNF-α is not as effective as IL-6 in protecting myeloma cells from H_2O_2-mediated oxidative cell death (Figure 3B).

Among intracellular antioxidant molecules, GSH is the most abundant non-protein thiol and constitutes the first-line defence against oxidative injury [33,34]. Furthermore, pro-inflammatory cytokines, such as IL-6 [35,36] and TNF-α [37], have been shown to regulate GSH synthesis in normal and cancer cells. We therefore investigated how the intracellular GSH pool in myeloma cells is perturbed by these cytokines. In 8226 cells, treatment with IL-6 (2.5 or 50 ng/ml) for 4 h resulted in a decrease in total intracellular GSH, whereas IL-6 treatment for 10 h or 24 h showed a trend towards an overall increase in the steady-state levels of GSH (Figure 3C). TNF-α treatment (2.5 or 10 ng/ml) resulted in a sustained decrease in GSH levels at 4, 10 and 24 h (Figure 3C). The GSH kinetics over time with IL-6 and TNF-α was repeated in MM.1S cells, where IL-6 treatment showed a transient early decrease in GSH levels, whereas TNF-α treatment showed decreased total GSH levels up to 24 h (results not shown).

Overall, Figure 3 shows that simultaneous treatment with IL-6 and H_2O_2 increases NF-κB activation, protects myeloma cells from H_2O_2-mediated oxidative cell death, and results in a transient early decrease in GSH levels. On the basis of results obtained with TNF-α, we speculate that TNF-α plus H_2O_2 treatment results in an overall oxidized intracellular environment in myeloma cells that could result in NF-κB inactivation. Indeed, studies have shown a complex redox regulation of NF-κB activation that can be modulated by multiple kinase(s) and phosphatase(s). Studies have shown that a reduced intracellular environment favours NF-κB activation [38], and redox changes mediated by TNF-α treatment can inhibit NF-κB activity [39].

IL-6 and IR treatment augment NF-κB activation, MnSOD activity and mRNA expression in myeloma cells

To understand IL-6-mediated therapy resistance in myeloma cells, we next determined whether treatments with IL-6 and/or IR leads to alterations in NF-κB activation as seen with IL-6 plus H_2O_2 treatment. In the NF-κB-luc assay, IR and IL-6 treatments independently increased transcriptional activity of NF-κB at 4 h, and this effect was increased additively with IL-6 plus IR (Figure 4A). Pre-incubation with NAC abrogated increases in NF-κB activity, suggesting that IL-6- and IR-mediated early activation of NF-κB were occurring by increased steady-state levels of pro-oxidants.

Previous studies have shown that an intronic NF-κB element is critical in driving expression of the *SOD2* mRNA [18]. MnSOD protein expression was thus determined after IL-6 (50 ng/ml) and/or IR treatments. For both MM.1S and 8226 cells, IL-6 or IR treatments increased MnSOD protein expression, which was further increased by IL-6 plus IR (Figure 4B). A dose–response curve with IL-6 (2.5 or 10 ng/ml) showed that the lower concentrations of IL-6 also induced MnSOD protein expression in myeloma cells (Supplementary Figure S4A at http://www.BiochemJ.org/bj/444/bj4440515add.htm).

To determine whether the increased MnSOD protein levels correspond to increased enzymatic activity, myeloma cells were treated with IL-6 and/or IR in the absence or presence of the NBD peptide (which inhibits NF-κB by targeting the IκB kinase complex). Treatments with IL-6 or IR induced an increase in MnSOD activity that was attenuated by NBD (Figure 4C). Furthermore, IL-6 plus IR treatment mediated an increase in MnSOD activity, which was significantly higher than that produced by IR alone, and was inhibited by NBD (Figure 4C). The NF-κB-inhibitory effect of NBD was confirmed using Ad-NF-κB-Luc reporter (Supplementary Figure S4B). NBD treatment was, however, found to attenuate both constitutive and ROS-induced MnSOD activity. To further confirm whether inducible NF-κB activity results in MnSOD up-regulation, Ad-IκBα-DN was used, which effectively inhibited IL-6- and IR-induced NF-κB activation (Supplementary Figure S4C) with a corresponding increase in IκBα protein expression (Supplementary Figure S4D).

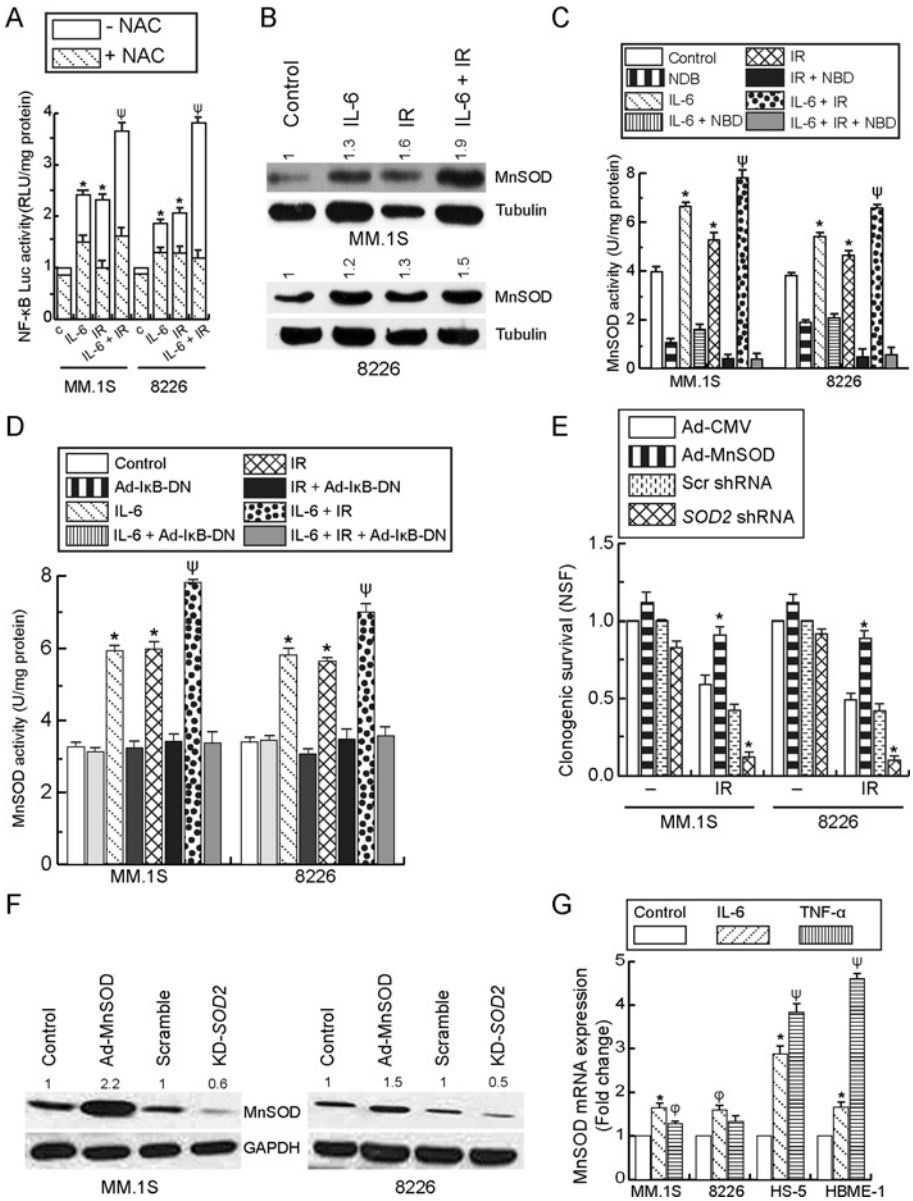

Figure 4 IL-6 and/or IR treatment results in NF-κB-driven MnSOD expression and clonogenic survival

(**A**) Myeloma cells were treated with IL-6 (50 ng/ml) and/or IR, and Luc activity was measured at 4 h. Results depict the mean RLU $\pm$ S.D., $n = 3$, normalized to protein concentration. $^{*}P < 0.05$ compared with the control, $^{\Psi}P < 0.005$ compared with IR treatment alone. (**B**) Myeloma cells were treated with IL-6 (50 ng/ml) and/or IR for 24 h and the whole-cell extract was probed with anti-MnSOD or anti-tubulin antibodies. The quantification of three independent experiments, expressed as the ratio between MnSOD and tubulin levels, after normalization to untreated control is shown above each band. MnSOD activity at 24 h after treatment with IL-6 (50 ng/ml) and/or IR (**C**) following pre-treatment with NBD (50 μM for 2 h) or (**D**) Ad-IκBα-DN (MOI = 10). Values are expressed as the mean $\pm$ S.D. for three replicates. $^{*}P < 0.001$ compared with the control, $^{\Psi}P < 0.001$ compared with IR treatment alone. (**E**) Myeloma cells with MnSOD overexpression or *SOD2* KD were analysed for clonogenic survival and data were normalized to untreated controls. Values are expressed as the mean $\pm$ S.D. for three replicates. $^{*}P < 0.005$ compared with control. (**F**) Characterization of myeloma cells by immunoblotting for MnSOD overexpression or KD. The quantification of three independent experiments, following normalization to the control, is shown above each band. (**G**) qPCR analysis was performed after exposure to IL-6 or TNF-α for 10 h. $^{*}P < 0.01$, $^{\varphi}P < 0.05$ and $^{\Psi}P < 0.001$ compared with the control.

Treatment with IL-6 and/or IR up-regulated MnSOD activity, which was significantly inhibited with Ad-IκBα-DN (Figure 4D). This result shows that ROS-induced NF-κB activation may be playing a direct role in up-regulating MnSOD activity in myeloma cells.

Clonogenic assays were performed to confirm the notion that increased MnSOD expression directly relates to radioresistance in myeloma cells. MnSOD overexpression increased clonogenicity of irradiated myeloma cells, and MnSOD KD significantly enhanced the radiosensitivity of both cell lines (Figure 4E). Alterations in MnSOD protein levels in Ad-MnSOD-transduced and stable *SOD2* KD cells were confirmed by immunoblotting (Figure 4F). The enzymatic activity of MnSOD was increased 10–15-fold with Ad-MnSOD (compared with the Ad-CMV control), whereas the activity was reduced 4–6-fold in *SOD2* KD cells (compared with cells expressing a scrambled control shRNA; results not shown).

As TNF-α and IL-1β are myeloma cell pro-proliferative cytokines that can also regulate MnSOD expression via NF-κB-mediated transcription [18], the relative ability of IL-6 and TNF-α to induce the *SOD2* mRNA expression was assessed. In myeloma cells, treatment with IL-6 or TNF-α showed an up-regulation of

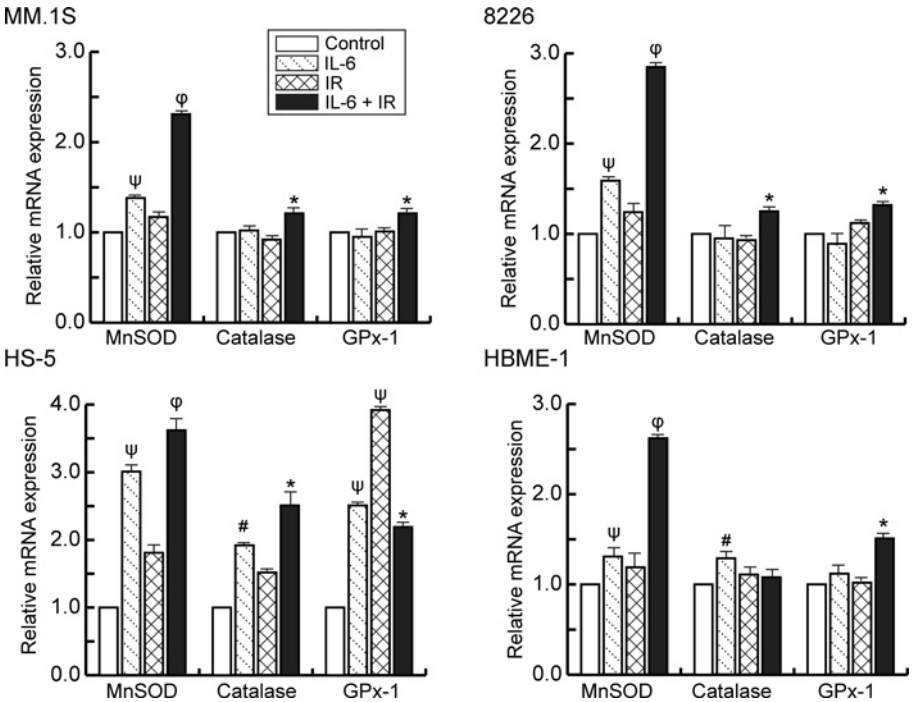

Figure 5 IL-6 increases levels of the *SOD2* mRNA and differentially regulates the mRNA levels of *CAT* and *GPx1*

Cells were treated with IL-6 (50 ng/ml) and/or IR, and qPCR analysis was performed to assess *SOD2*, *CAT* and *GPx1* mRNAs at 10 h. The results are presented as the fold change in mRNA expression relative to 18S mRNA, and are normalized to control untreated cells (mean of two independent experiments). $^{\Psi}P < 0.001$ and $^{\#}P < 0.01$ compared with control, $^{\varphi}P < 0.001$, $^{*}P < 0.05$ and $^{\varphi}P < 0.005$ compared with IR treatment alone.

SOD2 mRNA levels (Figure 4G). In HS-5 and HBME-1 cells, treatment with either IL-6 or TNF-α increased *SOD2* mRNA expression (Figure 4G). For myeloma cells, lower concentrations of IL-6 treatments (2.5 or 10 ng/ml) showed increased *SOD2* mRNA expression relative to untreated controls as measured by qPCR assay (results not shown). Taken together, the qPCR results show that IL-6 treatment up-regulates *SOD2* mRNA expression in myeloma cells, and both IL-6 or TNF-α treatments result in an increased expression of the *SOD2* mRNA in BM accessory cells that may potentially aid in myeloma cell survival and adaptation to oxidative stress. Steady-state levels of GSH in HS-5 and HBME-1 cells were measured as 70.4 and 57.2 nmol/mg of protein and were found to be higher than GSH levels in MM.1S and 8226 cells (25.9 and 32.3 nmol/mg of protein respectively, results not shown). Further studies are required to determine whether the endogenous higher thiol content renders a more robust increase in *SOD2* mRNA induction in the BM accessory cells.

Effect of IL-6 and irradiation on expression of mRNAs encoding antioxidant enzymes

In mammalian cells, the cellular defence against ROS includes enzymatic antioxidants, such as SODs, catalase and GPxs. We next determined if IL-6 treatment would alter IR-mediated perturbations in these antioxidant enzymes. Treatment with IL-6 up-regulated *SOD2* mRNA in all cells and IL-6 plus IR further increased the levels of *SOD2* transcripts (Figure 5). qPCR analysis of the major H_2O_2 detoxification enzymes, catalase and GPx-1, showed that, in myeloma cells, catalase or *GPx1* mRNA levels were not increased with IL-6, but were increased after combination treatment with IL-6 plus IR (Figure 5). In HS-5 cells, treatment with IL-6 caused a robust increase in *CAT* and *GPx1* mRNA, which was significantly increased with IL-6 plus IR treatment (Figure 5). Treatment with IL-6 increased *CAT* mRNA, and IL-6 plus IR induced *GPx1* mRNA in HBME-1 cells (Figure 5). From these qPCR results, it can be speculated that IL-6-mediated increases in levels of *SOD2*, *CAT* or *GPx1* mRNA probably helps in normalizing the level of oxidative stress induced by irradiation, thereby inducing radioresistance in myeloma cells and simultaneously preserving the myeloma cell microenvironment provided by the BM, and also secretion of paracrine cytokines; all of these events would be crucial in sustaining myeloma cell survival and proliferation following irradiation.

IL-6 inhibits mitochondrial oxidant production in myeloma cells

Since MnSOD closely regulates the clearance of ROS in the mitochondria and we observed an up-regulation of MnSOD by IL-6 treatment, flow cytometry was performed to detect IL-6- and/or IR-induced mitochondrial oxidant generation (presumably $O_2^{\bullet -}$) in myeloma cells [26]. For this, oxidation of the MitoSOX Red probe (a mitochondrially targeted hydroethidine derivative [28]) was utilized. At 36 h, treatment with IL-6 resulted in a trend towards a decrease in endogenous levels of mitochondrial oxidants with fold change as 0.5 ± 0.1 and 0.9 ± 0.1 for MM.1S and 8226 cells respectively relative to control untreated cells (set to 1.0). Irradiated cells showed elevated MitoSOX Red oxidation at 36 h (fold changes were 1.3 ± 0.3 and 2.7 ± 0.2 for MM.1S and 8226 cells respectively relative to untreated cells) that was significantly inhibited by IL-6 pre-treatment (fold changes were 0.8 ± 0.3 and 1.6 ± 0.2 for MM.1S and 8226 cells respectively, Figure 6A).

Live cell imaging of MitoSOX Red oxidation using confocal microscopy showed that, relative to the untreated control, IL-6

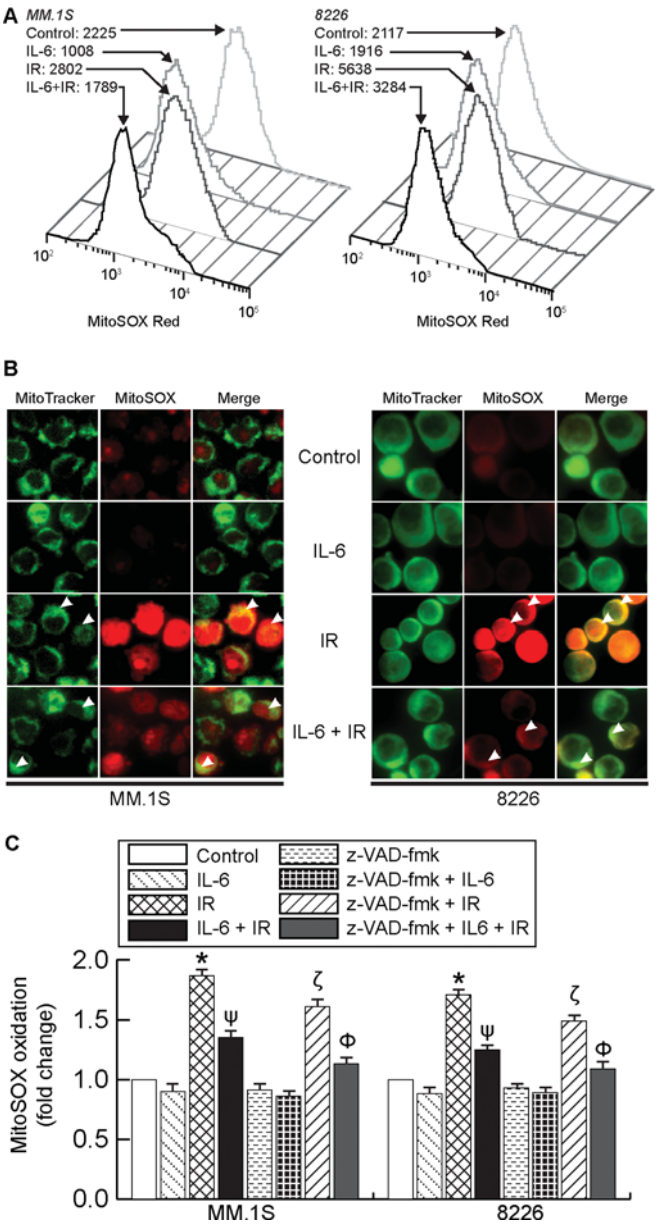

Figure 6 IL-6 attenuates irradiation-induced mitochondrial oxidant production

Myeloma cells were treated with IL-6 (50 ng/ml) and/or IR, and MitoSOX-derived red fluorescence was analysed at 36 h. (**A**) Measurement of MFI of oxidized MitoSOX Red by flow cytometry. Graphs with MFI values are shown from one experiment, and are representative of two independent experiments. For each graph, the *x* axis and *y* axis show the percentage of cells and MitoSOX oxidation respectively. (**B**) Confocal live imaging of MitoSOX Red and MitoTracker Green. Representative confocal images of control untreated cells and cells after IL-6 and/or IR treatments are shown. The 488 nm and 594 nm excitation wavelength was used for imaging MitoTracker Green and MitoSOX Red fluorescence signal respectively. Arrowheads point at significant alterations in MitoSOX-derived red fluorescence in mitochondria of IR and IL-6 plus IR treated myeloma cells. (**C**) Measurement of fluorescence intensity of oxidized MitoSOX in a plate reader assay. Cells were pre-treated without or with Z-VAD-FMK (100 μM for 2 h) followed by IL-6 and/or IR treatments. Data are presented as the fold change relative to the untreated control, and are representative of three independent experiments. $^{*}P < 0.005$ compared with control, $^{\Psi}P < 0.05$ compared with IR, $^{\zeta}P < 0.005$ compared with Z-VAD-FMK and $^{\varphi}P < 0.001$ compared with Z-VAD-FMK plus IR.

treatment resulted in a decrease in steady-state levels of mitochondrial oxidants, whereas irradiation caused a significant increase in MitoSOX Red oxidation as imaged at 36 h (Figure 6B). Furthermore, compared with IR alone, IL-6 plus IR treatment resulted in a remarkable reduction in steady-state levels of mitochondrial oxidants (Figure 6B). The specificity of MitoSOX oxidation was confirmed by treating the cells with antimycin A or PEG–SOD (results not shown).

Since the activation of caspases can result in feedback amplification of ROS production from mitochondria [40], the pan-caspase inhibitor Z-VAD-FMK was used to block ROS production by activated caspases, and MitoSOX oxidation was measured at 36 h following IL-6 and/or IR treatments. As shown in Figure 6(C), for both MM.1S and 8226 cells, irradiation resulted in an increased steady-state level of mitochondrial $O_2^{\bullet -}$ production that was significantly inhibited by IL-6 treatment. Inhibition of caspase activation partly attenuated irradiation-induced mitochondrial $O_2^{\bullet -}$ production, indicating the onset of late-phase ROS generated by caspase activation. Nevertheless, IL-6 treatment inhibited irradiation-induced MitoSOX oxidation in the presence of Z-VAD-FMK, confirming that IL-6-mediated early ROS is causally related to MnSOD-mediated attenuation of late mitochondrial oxidant production in irradiated myeloma cells. Taken together, MitoSOX Red oxidation results show that, in myeloma cells, IL-6 treatment attenuates endogenous and IR-induced increases in the steady-state levels of mitochondrial oxidants that would result in increased survival of myeloma cells to oxidative stressors.

DISCUSSION

MM remains a fatal disease, primarily owing to acquired resistance to anti-myeloma chemotherapeutic drugs [1]. Our previous studies have shown that combining targeted radiation with chemotherapeutic drugs enhances the effectiveness of radiotherapy in MM [10,20,24,41]. IL-6 is known to induce myeloma cell proliferation and confer aggressive growth properties and drug resistance in myeloma cells [1]. In myeloma and B-cell lymphoma, radioresistance has been correlated with the presence of IL-6-secreting tumour cells [42]. We previously reported that IR induces NF-κB activation in myeloma cells [23], and that paracrine IL-6 secretion confers radioresistance to myeloma cells [20]. Oxidative stressors such as IR and H_2O_2 have been shown to enhance IL-6 secretion by activating NF-κB transcription [43,44]. Thus IL-6 expression in the BM microenvironment is robust, and our published findings show that inhibition of constitutive and therapy-induced IL-6 synthesis is essential for effective killing of myeloma cells by IR. In the present study we evaluated the roles of myeloma-promoting cytokines, with a major focus on IL-6, in adaptation to endogenous and therapy-induced oxidative stress in myeloma and BM accessory cells.

Pro-inflammatory cytokines, such as TNF-α, IL-1β and IL-6 have been reported to induce $O_2^{\bullet -}$ production and also trigger downstream signalling events [3,30,45]. Using fluorigenic probes (H_2DCF-DA and DHE), the present study shows that IL-6 or TNF-α treatments induce a rapid rise in pro-oxidants in myeloma cells. With IL-6 treatment, HPLC analysis showed considerable formation of E^+ and other DHE oxidation products. Studies are ongoing to determine whether, in myeloma cells, DHE and 2-OH-E^+ rapidly reacts with different oxidants (such as H_2O_2 in the presence of haem proteins or peroxidases) and whether utilizing *SOD2* KD myeloma cells may aid in better identifying IL-6-induced $O_2^{\bullet -}$ production. Since both IL-6 and TNF-α directly induce myeloma cell proliferation and IL-1β drives paracrine IL-6 secretion, an increase in the production of ROS could mediate enhanced proliferation and the development of resistance to oxidative stressors. Notably, when IL-6 was combined with IR or Dex, a concerted increase in early ROS production was

observed. Since IL-6 treatment inhibited IR- and Dex-mediated myeloma cell death, IL-6 may play a role in the induction of redox-regulated antioxidant pathways in MM cells. Consistent with these findings, IL-6 has been shown to protect normal cells from injuries induced by oxidative stress [4,5,46].

IL-6 is a pro-proliferative cytokine for myeloma cells, and increased plasma levels of IL-6 correlates with poor prognosis [1]. On the basis of the disease stage, the serum levels of IL-6 in myeloma patients can range from 0.01 to 0.4 ng/ml; the actual IL-6 serum concentration can be even higher, since circulating IL-6 also binds to soluble IL-6 receptors [47]. In myelomatous BM, a local high concentration of IL-6 can be reached, given that myeloma cells produce IL-6 via the autocrine loop [48] and by adhesion with BM stromal cells, leading to paracrine IL-6 secretion by stromal cells [49]. In the present study we have combined exogenous IL-6 (50 ng/ml) with irradiation; however, lower concentrations of IL-6 (2.5 and 10 ng/ml) also protected myeloma cells from irradiation-induced apoptosis, resulted in pro-oxidant production and induced MnSOD protein expression. The protective effects of IL-6 on cell death induced by oxidative stressors were assessed after IL-6 pre-treatment for 6 h mainly because IL-6 showed maximum NF-κB activation at 4 h. Furthermore, as IL-6 is constantly present in the myeloma cell microenvironment, IL-6 treatment was continued until samples were collected for analysis. We plan to extend the present study to primary human myeloma samples in the near future. However, for *ex vivo* cultured primary myeloma cells, the culture medium is supplemented with exogenous IL-6 (5 ng/ml), making the experimental design difficult.

GSH provides a major source of thiol homoeostasis and constitutes the first line of the cellular defence mechanism against oxidative stressors. In cancer cells, increased GSH levels has been correlated with chemoresistance and radioresistance [33,50], and depletion of intracellular GSH can reverse drug resistance and improve the outcome of cancer therapies, including those for haematological malignancies [51,52]. GSH kinetics over time with IL-6 and TNF-α in myeloma cells show that IL-6 treatment results in a transient early decrease in GSH levels, whereas TNF-α treatment caused a more sustained decrease in total GSH levels until 24 h. Along similar lines, Nakajima et al. [36] showed that, in neuronal cells, IL-6 treatment results in increased γ-glutamylcysteine synthetase activity, which is the rate-limiting enzyme of GSH synthesis. Also, TNF-α treatment has been shown to decrease the intracellular levels of GSH by formation of mixed disulfides and inhibition of the glutathione reductase system [53,54]. Our ongoing studies will delineate how the thiol pool in myeloma cells is perturbed in the presence of various pro-inflammatory cytokines and if GSH depletion by buthionine sulfoximine would alter NF-κB activation and the overall therapy responses in multiple myeloma.

Previous studies have shown that under normal physiological conditions, i.e. when cells are able to maintain redox homoeostasis, ROS may function as intracellular signalling molecules [55] and ROS-mediated NF-κB activation regulates cellular redox homoeostasis [56]. NF-κB activation by oxidants is cell-context dependent and can be increased or decreased, depending on sequential events and concentrations of oxidants and antioxidants [57]. Studies have shown that a reduced intracellular environment favours NF-κB activation [38], and redox changes mediated by TNF-α treatment can inhibit NF-κB activity [39]. In myeloma cells, simultaneous treatment with IL-6 and H_2O_2 showed increased NF-κB activation, whereas TNF-α in combination with H_2O_2 inhibited NF-κB activity. TNF-α plays a role in MM pathogenesis by up-regulating NF-κB-induced expression of adhesion molecules on myeloma and BM stem cells, thus increasing paracrine IL-6-mediated MM cell growth and survival. In the present study, TNF-α was not as effective as IL-6 in protecting myeloma cells from H_2O_2-mediated oxidative myeloma cell death. Further studies are warranted to determine how TNF-α treatment regulates NF-κB activation in myeloma cells in the presence of oxidative stress-inducing therapies.

Mammalian cells possess a well-co-ordinated enzymatic antioxidant defence system comprised principally of SODs, catalase, peroxiredoxins and GPxs, and this system aids in rapid defence against oxidative stress. In myeloma cells, the present study provides evidence for NF-κB to play a role in driving IL-6-mediated up-regulation of MnSOD expression, and shows that IL-6 treatment leads to increases in the enzymatic activity of MnSOD. Furthermore, IL-6-induced NF-κB activation rendered radioresistance in myeloma cells. Indeed, MnSOD is a potent protector of cancer cells against both chemotherapy and radiotherapy [58,59]. Also, TNF-α, IL-1β and IL-6 treatments can increase MnSOD expression [60–63], and NF-κB-mediated *SOD*2 transcription has been associated with cytokine and IR treatments [18,30,31]. Previous studies have identified a clear role of NF-κB in *IL6* gene expression [64]. Further studies will determine whether a feed-forward loop of NF-κB on IL-6 signalling is responsible for a stronger effect on MnSOD activity. Indeed, improved myeloma cell cytotoxicity was seen when 2-methoxyestradiol, a proposed inhibitor of MnSOD, was combined with ROS-generating drugs, such as bortezomib [65] and arsenic trioxide [66]. In myeloma cells, IL-6-mediated MnSOD up-regulation was partially coupled with increases in the mRNA levels of *CAT* and *GPx1*. Thus induction of MnSOD by IL-6 treatment may potentially lead to a transient accumulation of H_2O_2 in myeloma cells that may be alleviated by the up-regulation of hydroperoxide-metabolizing systems.

During basal steady-state metabolism, ROS are generated primarily from mitochondrial respiratory chains, and mitochondria are believed to serve as a nodal control point that regulates apoptosis. Furthermore, antioxidant systems, such as glutathione/GPx and MnSOD, work dynamically to regulate any endogenous and/or therapy-induced elevation of mitochondrial ROS, and to inhibit apoptosis initiated by oxidative damage to mitochondria. The present study shows that treatment with IL-6 decreases IR-induced late mitochondrial pro-oxidant generation in myeloma cells, suggesting that, besides providing pro-proliferative signalling, IL-6 may inhibit IR- and chemotherapy-induced oxidative damage to the mitochondria of myeloma cells.

In conclusion, the resistance of several haemopoietic cancers to cytotoxic chemotherapy and radiotherapy is well established but not understood. The present study provides evidence to support a role for IL-6 in myeloma therapy resistance and proposes a mechanism involving NF-κB-dependent up-regulation of MnSOD. Our results provide a novel biochemical rationale for combining MnSOD inhibition with oxidative stress-inducing therapeutic agents, which paradoxically also stimulate IL-6 and thereby counteract oxidative stress, for the development of an effective new therapeutic strategy for treating MM.

AUTHOR CONTRIBUTION

Charles Brown and Kelley Salem performed the experiments and analysed the results. Soumen Bera provided technical assistance with Western blotting and a few other assays. Neeraj Singh helped with the GSH studies. Brett Wagner conducted HPLC studies and Garry Buettner provided expertise in interpretation of HPLC results. Ajit Tiwari performed confocal microscopy and Amit Choudhury provided expertise in ROS estimation by confocal imaging. Apollina Goel conceptualized the study, oversaw the experiments and results, and co-wrote the paper with the other authors.

FUNDING

This work was supported by the National Institutes of Health [grant numbers CA127958 and P30CA086862 (to A.G.), T32CA078586 (to K.S.), HL089599 (to A.C.) and GM073929 (to G.R.B.)].

ACKNOWLEDGEMENTS

We thank the Radiation and Free Radical Research Core Facility and Justin Fishbaugh in Flow Cytometry Core Facility (The University of Iowa, P30CA086862) for their services. We thank the Domann laboratory for technical advice on qPCR, Dr Michael L. McCormick for technical advice on estimating SOD and GSH levels and Jessica Olson for technical assistance with experiments. We also thank Dr Christine Blaumueller for editorial help and Gareth Smith for editing illustrations prior to submission.

REFERENCES

1 Hideshima, T., Mitsiades, C., Tonon, G., Richardson, P. G. and Anderson, K. C. (2007) Understanding multiple myeloma pathogenesis in the bone marrow to identify new therapeutic targets. Nat. Rev. Cancer **7**, 585–598
2 Kharazmi, A., Nielsen, H., Rechnitzer, C. and Bendtzen, K. (1989) Interleukin 6 primes human neutrophil and monocyte oxidative burst response. Immunol. Lett. **21**, 177–184
3 Behrens, M. M., Ali, S. S. and Dugan, L. L. (2008) Interleukin-6 mediates the increase in NADPH-oxidase in the ketamine model of schizophrenia. J. Neurosci. **28**, 13957–13966
4 Sun, Z., Klein, A. S., Radaeva, S., Hong, F., El-Assal, O., Pan, H. N., Jaruga, B., Batkai, S., Hoshino, S., Tian, Z. et al. (2003) *In vitro* interleukin-6 treatment prevents mortality associated with fatty liver transplants in rats. Gastroenterology **125**, 202–215
5 Ward, N. S., Waxman, A. B., Homer, R. J., Mantell, L. L., Einarsson, O., Du, Y. and Elias, J. A. (2000) Interleukin-6-induced protection in hyperoxic acute lung injury. Am. J. Respir. Cell Mol. Biol. **22**, 535–542
6 Fruehauf, J. P. and Meyskens, Jr, F. L. (2007) Reactive oxygen species: a breath of life or death? Clin. Cancer Res. **13**, 789–794
7 Kuku, I., Aydogdu, I., Bayraktar, N., Kaya, E., Akyol, O. and Erkurt, M. A. (2005) Oxidant/antioxidant parameters and their relationship with medical treatment in multiple myeloma. Cell Biochem. Funct. **23**, 47–50
8 Sharma, A., Tripathi, M., Satyam, A. and Kumar, L. (2009) Study of antioxidant levels in patients with multiple myeloma. Leuk. Lymphoma **50**, 809–815
9 Zima, T., Spicka, I., Stipek, S., Crkovska, J., Platenik, J., Merta, M., Nemecek, K. and Tesar, V. (1996) [Lipid peroxidation and activity of antioxidative enzymes in patients with multiple myeloma]. Cas. Lek. Cesk. **135**, 14–17
10 Goel, A., Spitz, D. R. and Weiner, G. J. (2011) Manipulation of cellular redox metabolism for improving therapeutic responses in B-cell lymphoma and multiple myeloma. J. Cell. Biochem. **113**, 419–425
11 Weisiger, R. A. and Fridovich, I. (1973) Superoxide dismutase. Organelle specificity. J. Biol. Chem. **248**, 3582–3592
12 Oberley, L. W. (2001) Anticancer therapy by overexpression of superoxide dismutase. Antioxid. Redox Signaling **3**, 461–472
13 Van Remmen, H., Ikeno, Y., Hamilton, M., Pahlavani, M., Wolf, N., Thorpe, S. R., Alderson, N. L., Baynes, J. W., Epstein, C. J., Huang, T. T. et al. (2003) Life-long reduction in MnSOD activity results in increased DNA damage and higher incidence of cancer but does not accelerate aging. Physiol. Genomics **16**, 29–37
14 Hodge, D. R., Peng, B., Pompeia, C., Thomas, S., Cho, E., Clausen, P. A., Marquez, V. E. and Farrar, W. L. (2005) Epigenetic silencing of manganese superoxide dismutase (SOD-2) in KAS 6/1 human multiple myeloma cells increases cell proliferation. Cancer Biol. Ther. **4**, 585–592
15 Hurt, E. M., Thomas, S. B., Peng, B. and Farrar, W. L. (2007) Integrated molecular profiling of SOD2 expression in multiple myeloma. Blood **109**, 3953–3962
16 Flohe, L., Brigelius-Flohe, R., Saliou, C., Traber, M. G. and Packer, L. (1997) Redox regulation of NF-κB activation. Free Radical Biol. Med. **22**, 1115–1126
17 Demchenko, Y. N. and Kuehl, W. M. (2010) A critical role for the NFkB pathway in multiple myeloma. Oncotarget **1**, 59–68
18 Xu, Y., Kiningham, K. K., Devalaraja, M. N., Yeh, C. C., Majima, H., Kasarskis, E. J. and St Clair, D. K. (1999) An intronic NF-κB element is essential for induction of the human manganese superoxide dismutase gene by tumor necrosis factor-α and interleukin-1β. DNA Cell Biol. **18**, 709–722
19 Li, Q. and Engelhardt, J. F. (2006) Interleukin-1β induction of NFκB is partially regulated by H_2O_2-mediated activation of NFκB-inducing kinase. J. Biol. Chem. **281**, 1495–1505
20 Bera, S., Greiner, S., Choudhury, A., Dispenzieri, A., Spitz, D. R., Russell, S. J. and Goel, A. (2010) Dexamethasone-induced oxidative stress enhances myeloma cell radiosensitization while sparing normal bone marrow hematopoiesis. Neoplasia **12**, 980–992
21 Puck, T. T., Marcus, P. I. and Cieciura, S. J. (1956) Clonal growth of mammalian cells *in vitro*: growth characteristics of colonies from single HeLa cells with and without a feeder layer. J. Exp. Med. **103**, 273–283
22 Jules Mattes, M. (2005) High-sensitivity cytotoxicity assays for nonadherent cells. Methods Mol. Med. **110**, 29–37
23 Goel, A., Dispenzieri, A., Greipp, P. R., Witzig, T. E., Mesa, R. A. and Russell, S. J. (2005) PS-341-mediated selective targeting of multiple myeloma cells by synergistic increase in ionizing radiation-induced apoptosis. Exp. Hematol. **33**, 784–795
24 Goel, A., Dispenzieri, A., Geyer, S. M., Greiner, S., Peng, K. W. and Russell, S. J. (2006) Synergistic activity of the proteasome inhibitor PS-341 with non-myeloablative 153-Sm-EDTMP skeletally targeted radiotherapy in an orthotopic model of multiple myeloma. Blood **107**, 4063–4070
25 Zielonka, J., Hardy, M. and Kalyanaraman, B. (2009) HPLC study of oxidation products of hydroethidine in chemical and biological systems: ramifications in superoxide measurements. Free Radical Biol. Med. **46**, 329–338
26 Zhao, H., Joseph, J., Fales, H. M., Sokoloski, E. A., Levine, R. L., Vasquez-Vivar, J. and Kalyanaraman, B. (2005) Detection and characterization of the product of hydroethidine and intracellular superoxide by HPLC and limitations of fluorescence. Proc. Natl. Acad. Sci. U.S.A. **102**, 5727–5732
27 Nakao, T., Kim, S., Ohta, K., Kawano, H., Hino, M., Miura, K., Tatsumi, N. and Iwao, H. (2002) Role of mitogen-activated protein kinase family in serum-induced leukaemia inhibitory factor and interleukin-6 secretion by bone marrow stromal cells. Br. J. Pharmacol. **136**, 975–984
28 Robinson, K. M., Janes, M. S., Pehar, M., Monette, J. S., Ross, M. F., Hagen, T. M., Murphy, M. P. and Beckman, J. S. (2006) Selective fluorescent imaging of superoxide *in vivo* using ethidium-based probes. Proc. Natl. Acad. Sci. U.S.A. **103**, 15038–15043
29 Zielonka, J. and Kalyanaraman, B. (2010) Hydroethidine- and MitoSOX-derived red fluorescence is not a reliable indicator of intracellular superoxide formation: another inconvenient truth. Free Radical Biol. Med. **48**, 983–1001
30 Brigelius-Flohe, R., Banning, A., Kny, M. and Bol, G. F. (2004) Redox events in interleukin-1 signaling. Arch. Biochem. Biophys. **423**, 66–73
31 Morgan, M. J. and Liu, Z. G. (2010) Reactive oxygen species in TNFα-induced signaling and cell death. Mol. Cells **30**, 1–12
32 Cadenas, E. (1989) Biochemistry of oxygen toxicity. Annu. Rev. Biochem. **58**, 79–110
33 Estrela, J. M., Ortega, A. and Obrador, E. (2006) Glutathione in cancer biology and therapy. Crit. Rev. Clin. Lab. Sci. **43**, 143–181
34 Schafer, F. Q. and Buettner, G. R. (2001) Redox environment of the cell as viewed through the redox state of the glutathione disulfide/glutathione couple. Free Radical Biol. Med. **30**, 1191–1212
35 Hack, V., Gross, A., Kinscherf, R., Bockstette, M., Fiers, W., Berke, G. and Droge, W. (1996) Abnormal glutathione and sulfate levels after interleukin 6 treatment and in tumor-induced cachexia. FASEB J. **10**, 1219–1226
36 Nakajima, A., Yamada, K., Zou, L. B., Yan, Y., Mizuno, M. and Nabeshima, T. (2002) Interleukin-6 protects PC12 cells from 4-hydroxynonenal-induced cytotoxicity by increasing intracellular glutathione levels. Free Radical Biol. Med. **32**, 1324–1332
37 Urata, Y., Yamamoto, H., Goto, S., Tsushima, H., Akazawa, S., Yamashita, S., Nagataki, S. and Kondo, T. (1996) Long exposure to high glucose concentration impairs the responsive expression of γ-glutamylcysteine synthetase by interleukin-1β and tumor necrosis factor-α in mouse endothelial cells. J. Biol. Chem. **271**, 15146–15152
38 Korn, S. H., Wouters, E. F., Vos, N. and Janssen-Heininger, Y. M. (2001) Cytokine-induced activation of nuclear factor-κB is inhibited by hydrogen peroxide through oxidative inactivation of IκB kinase. J. Biol. Chem. **276**, 35693–35700
39 Han, D., Hanawa, N., Saberi, B. and Kaplowitz, N. (2006) Hydrogen peroxide and redox modulation sensitize primary mouse hepatocytes to TNF-induced apoptosis. Free Radical Biol. Med. **41**, 627–639
40 Chen, Q., Chai, Y. C., Mazumder, S., Jiang, C., Macklis, R. M., Chisolm, G. M. and Almasan, A. (2003) The late increase in intracellular free radical oxygen species during apoptosis is associated with cytochrome *c* release, caspase activation, and mitochondrial dysfunction. Cell Death Differ. **10**, 323–334
41 Goel, A. and Russell, S. J. (2006) Enhancing the therapeutic index of radiation in multiple myeloma. Drug Discovery Today **3**, 515–522
42 Gougelet, A., Mansuy, A., Blay, J. Y., Alberti, L. and Vermot-Desroches, C. (2009) Lymphoma and myeloma cell resistance to cytotoxic agents and ionizing radiations is not affected by exposure to anti-IL-6 antibody. PLoS ONE **4**, e8026
43 Beetz, A., Messer, G., Oppel, T., van Beuningen, D., Peter, R. U. and Kind, P. (1997) Induction of interleukin 6 by ionizing radiation in a human epithelial cell line: control by corticosteroids. Int. J. Radiat. Biol. **72**, 33–43
44 Zhang, J., Johnston, G., Stebler, B. and Keller, E. T. (2001) Hydrogen peroxide activates NFκB and the interleukin-6 promoter through NFκB-inducing kinase. Antioxid. Redox Signaling **3**, 493–504
45 Morgan, M. J., Kim, Y. S. and Liu, Z. G. (2008) TNFα and reactive oxygen species in necrotic cell death. Cell Res. **18**, 343–349

46 Kida, H., Yoshida, M., Hoshino, S., Inoue, K., Yano, Y., Yanagita, M., Kumagai, T., Osaki, T., Tachibana, I., Saeki, Y. and Kawase, I. (2005) Protective effect of IL-6 on alveolar epithelial cell death induced by hydrogen peroxide. Am. J. Physiol. Lung Cell Mol. Physiol. **288**, L342–L349

47 Klein, B., Zhang, X. G., Lu, Z. Y. and Bataille, R. (1995) Interleukin-6 in human multiple myeloma. Blood **85**, 863–872

48 Frassanito, M. A., Cusmai, A., Iodice, G. and Dammacco, F. (2001) Autocrine interleukin-6 production and highly malignant multiple myeloma: relation with resistance to drug-induced apoptosis. Blood **97**, 483–489

49 Uchiyama, H., Barut, B. A., Mohrbacher, A. F., Chauhan, D. and Anderson, K. C. (1993) Adhesion of human myeloma-derived cell lines to bone marrow stromal cells stimulates interleukin-6 secretion. Blood **82**, 3712–3720

50 Dethmers, J. K. and Meister, A. (1981) Glutathione export by human lymphoid cells: depletion of glutathione by inhibition of its synthesis decreases export and increases sensitivity to irradiation. Proc. Natl. Acad. Sci. U.S.A. **78**, 7492–7496

51 Takahashi, S. (2010) Combination therapy with arsenic trioxide for hematological malignancies. Anticancer Agents Med. Chem. **10**, 504–510

52 Bates, S. E., Regis, J. I., Robey, R. W., Zhan, Z., Scala, S. and Meadows, B. J. (1994) Chemoresistance in the clinic: overview 1994. Bull. Cancer **81** (Suppl. 2), 55s–61s

53 Bellomo, G., Mirabelli, F., DiMonte, D., Richelmi, P., Thor, H., Orrenius, C. and Orrenius, S. (1987) Formation and reduction of glutathione-protein mixed disulfides during oxidative stress. A study with isolated hepatocytes and menadione (2-methyl-1,4-naphthoquinone). Biochem. Pharmacol. **36**, 1313–1320

54 Ishii, Y., Partridge, C. A., Del Vecchio, P. J. and Malik, A. B. (1992) Tumor necrosis factor-α-mediated decrease in glutathione increases the sensitivity of pulmonary vascular endothelial cells to H_2O_2. J. Clin. Invest. **89**, 794–802

55 Trachootham, D., Lu, W., Ogasawara, M. A., Nilsa, R. D. and Huang, P. (2008) Redox regulation of cell survival. Antioxid. Redox Signaling **10**, 1343–1374

56 Morgan, M. J. and Liu, Z. G. Crosstalk of reactive oxygen species and NF-κB signaling. Cell Res. **21**, 103–115

57 Acharya, A., Das, I., Chandhok, D. and Saha, T. (2010) Redox regulation in cancer: a double-edged sword with therapeutic potential. Oxid. Med. Cell. Longev. **3**, 23–34

58 Hirose, K., Longo, D. L., Oppenheim, J. J. and Matsushima, K. (1993) Overexpression of mitochondrial manganese superoxide dismutase promotes the survival of tumor cells exposed to interleukin-1, tumor necrosis factor, selected anticancer drugs, and ionizing radiation. FASEB J. **7**, 361–368

59 Motoori, S., Majima, H. J., Ebara, M., Kato, H., Hirai, F., Kakinuma, S., Yamaguchi, C., Ozawa, T., Nagano, T., Tsujii, H. and Saisho, H. (2001) Overexpression of mitochondrial manganese superoxide dismutase protects against radiation-induced cell death in the human hepatocellular carcinoma cell line HLE. Cancer Res. **61**, 5382–5388

60 Bissonnette, C. J., Klegeris, A., McGeer, P. L. and McGeer, E. G. (2004) Interleukin 1α and interleukin 6 protect human neuronal SH-SY5Y cells from oxidative damage. Neurosci. Lett. **361**, 40–43

61 Isoherranen, K., Peltola, V., Laurikainen, L., Punnonen, J., Laihia, J., Ahotupa, M. and Punnonen, K. (1997) Regulation of copper/zinc and manganese superoxide dismutase by UVB irradiation, oxidative stress and cytokines. J. Photochem. Photobiol. B. **40**, 288–293

62 Mathy-Hartert, M., Hogge, L., Sanchez, C., Deby-Dupont, G., Crielaard, J. M. and Henrotin, Y. (2008) Interleukin-1β and interleukin-6 disturb the antioxidant enzyme system in bovine chondrocytes: a possible explanation for oxidative stress generation. Osteoarthritis Cartilage **16**, 756–763

63 Ono, M., Kohda, H., Kawaguchi, T., Ohhira, M., Sekiya, C., Namiki, M., Takeyasu, A. and Taniguchi, N. (1992) Induction of Mn-superoxide dismutase by tumor necrosis factor, interleukin-1 and interleukin-6 in human hepatoma cells. Biochem. Biophys. Res. Commun. **182**, 1100–1107

64 Chiang, M. Y. and Stadtmauer, E. A. (2004) NF-κB, IL-6 and myeloma cell growth: making the connection. Cancer Biol. Ther. **3**, 1018–1020

65 Chauhan, D., Li, G., Auclair, D., Hideshima, T., Podar, K., Mitsiades, N., Mitsiades, C., Chen, L. B., Munshi, N., Saxena, S. and Anderson, K. C. (2004) 2-Methoxyestradiol and bortezomib/proteasome-inhibitor overcome dexamethasone-resistance in multiple myeloma cells by modulating heat shock protein-27. Apoptosis **9**, 149–155

66 Zhou, L., Hou, J., Fu, W., Wang, D., Yuan, Z. and Jiang, H. (2008) Arsenic trioxide and 2-methoxyestradiol reduce β-catenin accumulation after proteasome inhibition and enhance the sensitivity of myeloma cells to bortezomib. Leuk. Res. **32**, 1674–1683

Received 17 November 2011/12 March 2012; accepted 3 April 2012
Published as BJ Immediate Publication 3 April 2012, doi:10.1042/BJ20112019

Biochem. J. (2012) **444**, 515–527 (Printed in Great Britain) doi:10.1042/BJ20112019

online data

SUPPLEMENTARY ONLINE DATA

Interleukin-6 counteracts therapy-induced cellular oxidative stress in multiple myeloma by up-regulating manganese superoxide dismutase

Charles O. BROWN*[1], Kelley SALEM*[1], Brett A. WAGNER*, Neeraj SINGH*, Ajit TIWARI†, Amit CHOUDHURY†, Garry R. BUETTNER* and Apollina GOEL*[2]

*Free Radical and Radiation Biology Program, Department of Radiation Oncology, University of Iowa, Iowa City, IA 52242, U.S.A., and †Department of Anatomy and Cell Biology, The Holden Comprehensive Cancer Center, University of Iowa, Iowa City, IA 52242, U.S.A.

EXPERIMENTAL

Cytotoxicity analysis using MTT assay

Cells were seeded in 96-well plates and a subset was pretreated with IL-6 (50 ng/ml). Cells were subsequently treated with Dex (1 μM) or irradiation (6 Gy) and cultured for 48 h. Cell viability and proliferation was assessed with MTT dye using a commercially available kit (A.T.C.C.) [1,2].

HPLC analysis of DHE oxidation products

For quantitative analysis of DHE oxidation products, HPLC electrochemical analysis was performed [3,4]. Briefly, 8226 cells (1×10^6 cells/condition) were preloaded with DHE (10 μM at 37 °C for 30 min), followed by treatment with IL-6 (50 ng/ml) or antimycin A (10 μM), or no treatment (control) for 30 min. Cells were centrifuged, washed with PBS, counted and stored at − 80 °C. On the day of HPLC analysis, samples were prepared as described by Zielonka et al. [3]. An ESA CoulArray system with a Phenomenex 250 mm×4.6 mm Synergi 4 μm Polar-RP 80A column was used to quantify oxidation products of DHE. Quantification of 2-OH-E^+ was determined using the 200, 280 and 365 mV channels, and E^+, using the 280, 365, 400, 450 and 500 mV channels and standard curves were prepared from authentic standards. HPLC data were adjusted for cell numbers and dilutions made during sample processing and analysis.

NF-κB assay

The transcriptional activity of NF-κB was measured using an ELISA-based assay (TransAM NF-κB p65 transcription factor assay kit) as described previously [5]. Cells were infected with or without Ad-IκBα-DN for 48 h and exposed to 6-Gy IR or sham IR. Nuclear extracts were prepared 2 h after IR and incubated with immobilized oligonucleotide containing a consensus-binding site for the p65 subunit of NF-κB or the control oligonucleotide. Binding was detected by a primary antibody specific for p65 followed by incubation with anti-IgG antibody conjugated to horseradish peroxidase. The product was quantified at 450 nm. Absorbance of the untreated cells was set to 1 and the fold activation/repression in the NF-κB activity was evaluated after normalizing the samples for cellular protein content.

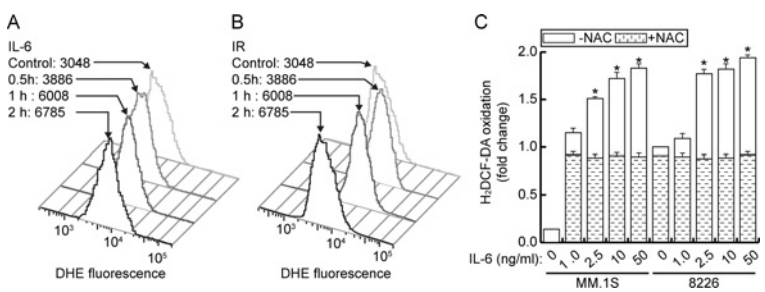

Figure S1 Treatment with IL-6 or IR induces early ROS production in MM.1S myeloma cells

MM.1S cells were treated for 0.5, 1 or 2 h with (**A**) IL-6 or (**B**) IR, and DHE oxidation was measured by flow cytometry. Graphs with MFI values are shown from one experiment, and are representative of two experiments. (**C**) Myeloma cells were pretreated without or with NAC, and then incubated with IL-6 (1, 2.5, 10 or 50 ng/ml) and H_2DCF-DA oxidation was measured at 2 h. *$P < 0.05$ compared with control (no IL-6 treatment).

[1] These authors contributed equally to this study.
[2] To whom correspondence should be addressed (email apollina-goel@uiowa.edu).

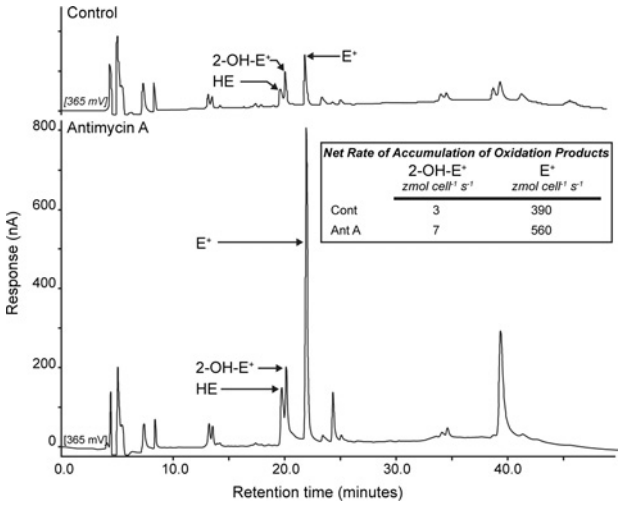

Figure S2 2-OH-E$^+$, the superoxide-derived oxidation product of DHE, is observed with HPLC

Representative HPLC chromatograms from 8226 cells incubated with DHE and then treated with antimycin A (Ant A) or untreated (control; Cont) for an additional 30 min. For simplicity, one channel (365 mV) of the eight channels monitored is presented to illustrate retention times and relative intensities of the various oxidation products of DHE found in cell extracts. HE is dihydroethidine, 2-OH-E$^+$ is the $O_2^{\bullet -}$ -specific 2-hydroxyethidium product, and E$^+$ is the non-specific two-electron oxidation product, ethidium. HPLC with electrochemical detection was performed using an ESA CoulArray system with a Phenomenex 250 mm $\times$ 4.6 mm Synergi 4 μm Polar-RP 80A column. Quantification of 2-OH-E$^+$ was determined using the 200, 280 and 365 mV channels, and E$^+$ was determined using the 280, 365, 400, 450 and 500 mV channels, and standard curves were prepared from authentic standards. The Table (inset) provides estimates of net rates of accumulation of the oxidation products in cells during experiments on a per cell basis; zmol is zeptomoles (10^{-21}).

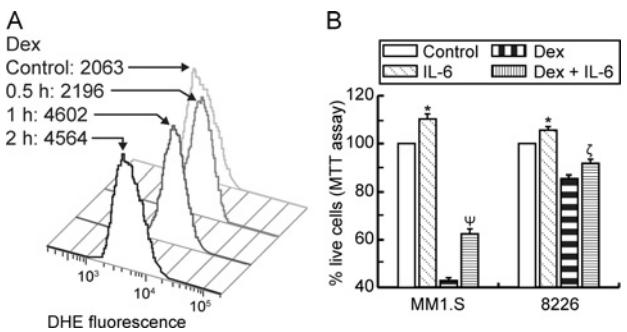

Figure S3 Dex induces early ROS production in MM.1S myeloma cells and IL-6 protects myeloma cells against Dex-induced cytotoxicity

(**A**) MM.1S cells were treated for 0.5, 1 or 2 h with Dex and DHE oxidation was measured by flow cytometry. For each graph depicting MFI, the *x* axis and *y* axis show the percentage of cells and DHE oxidation respectively. MFI values are shown from one experiment. (**B**) The MTT cell viability assay was performed after treatment with IL-6 and/or Dex. The data are expressed as the percentage of live cells relative to the untreated control, which is set at 100. $^*P < 0.05$ compared with control, and $^\zeta P < 0.01$ and $^\Psi P < 0.0001$ compared with Dex.

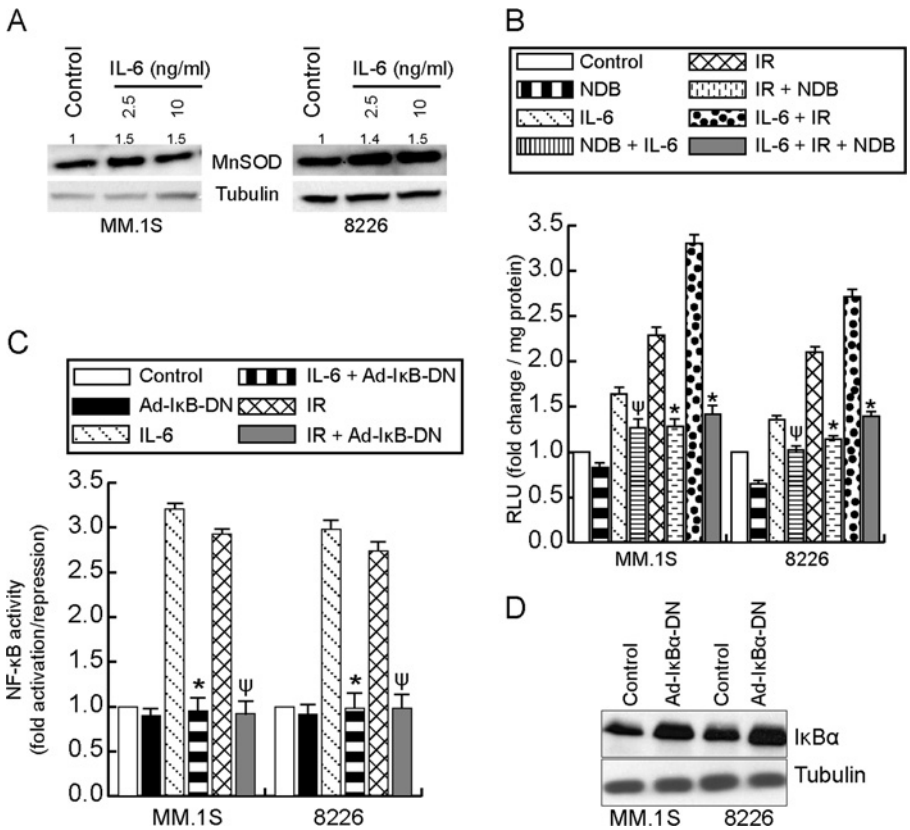

Figure S4 IL-6 treatment increases MnSOD expression and NBD and Ad-IκBα-DN inhibit NF-κB activity in myeloma cells

MM.1S and 8226 cells were treated with (**A**) IL-6 (2.5 or 10 ng/ml) and whole-cell extract was probed for MnSOD expression at 24 h. The ratio between MnSOD and tubulin levels, after normalization to untreated control, is shown above each band. Myeloma cells were treated with IL-6 (50 ng/ml) and/or IR (**B**) after pretreatment without or with NBD (50 μM for 2 h). Luc activity was measured at 4 h. Values are depicted as the fold change in mean RLU $\pm$ S.D., $n = 3$, normalized to protein concentration. $^{*}P < 0.01$ compared with IL-6, $^{\Psi}P < 0.01$ compared with IR treatment alone or IL-6 plus IR. Myeloma cells were treated with IL-6 (50 ng/ml) and/or IR (**C**) after 48 h of transduction with Ad-IκBα-DN (MOI = 10). The DNA-binding activity of NF-κB was analysed at 2 h in nuclear extracts. The results are presented as the fold repression or activation of NF-κB activity compared with control. $^{*}P < 0.01$ and $^{\Psi}P < 0.01$ compared with IR treatment alone. (**D**) Myeloma cells were transduced with Ad-IκBα-DN (MOI = 10), whole-cell extract was made at 48 h and probed with an antibody against IκBα or tubulin.

REFERENCES

1 Bera, S., Greiner, S., Choudhury, A., Dispenzieri, A., Spitz, D. R., Russell, S. J. and Goel, A. (2010) Dexamethasone-induced oxidative stress enhances myeloma cell radiosensitization while sparing normal bone marrow hematopoiesis. Neoplasia **12**, 980–992
2 Goel, A. and Russell, S. J. (2006) Enhancing the therapeutic index of radiation in multiple myeloma. Drug Discovery Today **3**, 515–522
3 Zielonka, J., Hardy, M. and Kalyanaraman, B. (2009) HPLC study of oxidation products of hydroethidine in chemical and biological systems: ramifications in superoxide measurements. Free Radical Biol. Med. **46**, 329–338
4 Zhao, H., Joseph, J., Fales, H. M., Sokoloski, E. A., Levine, R. L., Vasquez-Vivar, J. and Kalyanaraman, B. (2005) Detection and characterization of the product of hydroethidine and intracellular superoxide by HPLC and limitations of fluorescence. Proc. Natl. Acad. Sci. U.S.A. **102**, 5727–5732
5 Goel, A., Dispenzieri, A., Greipp, P. R., Witzig, T. E., Mesa, R. A. and Russell, S. J. (2005) PS-341-mediated selective targeting of multiple myeloma cells by synergistic increase in ionizing radiation-induced apoptosis. Exp. Hematol. **33**, 784–795

Received 17 November 2011/12 March 2012; accepted 3 April 2012
Published as BJ Immediate Publication 3 April 2012, doi:10.1042/BJ20112019